Spring 2012

Multibody dynamics of mechanism with secondary system

Jun Hyeak Choi
University of Iowa

MULTIBODY DYNAMICS OF MECHANISM WITH SECONDARY SYSTEM

by

Jun Hyeak Choi

A thesis submitted in partial fulfillment
of the requirements for the
Master of Science degree in Civil and Environmental Engineering
in the Graduate College of
The University of Iowa

May 2012

Thesis Supervisor: Professor Jasbir S. Arora
Assistant Research Engineer Rajan Bhatt

Graduate College
The University of Iowa
Iowa City, Iowa

CERTIFICATE OF APPROVAL

MASTER'S THESIS

This is to certify that the Master's thesis of

Jun Hyeak Choi

has been approved by the Examining Committee
for the thesis requirement for Master of
Science degree in Civil and Environmental Engineering
at the May 2012 graduation.

Thesis Committee: _____
Jasbir S. Arora, Thesis Supervisor

_____
Rajan Bhatt, Thesis Supervisor

_____
Karim Abdel-Malek

_____
Salam Rahmatalla

To my mother and grandmother who always support me with constant love and pray,
my wife who is the anchor of my life
and the memory of my father

ABSTRACT

Recent advances in predictive dynamics allow the user to not only predict physics based human motion simulations but also determine the actuation torques required to achieve those motions. The predictive dynamics approach uses optimization to predict motion while using many task based, physics based, and environment based constraints including the equations of motion. Many tasks have been simulated using this new method of predicting and simulating digital human motion, e.g. walking, running, stair climbing, and box lifting. In this research, we develop a method to predict the motion as well as effect of external equipment hanging on the digital human. The proposed method is tested on a simple case of a two degree of freedom serial chain mechanism with a simple passive system to behave as external equipment. In particular, the passive mass is assumed to be attached to the two links system with a spring and damper. Three different initial position cases are developed and tested to calculate motion and reaction force of spring and damper system. The results of the proposed method are compared with the results obtained by integrating the equations of motion of the full three degree of freedom system.

TABLE OF CONTENTS

LIST OF TABLES

LIST OF FIGURES

CHAPTER 1

INTRODUCTION

Digital human modeling and simulation has been an active research topic for the past two decades and has impacted the development and testing of new designs of products in many different fields. Being able to perform efficient static and dynamic analysis of human motion is a key element in developing a high-fidelity human model. Considering the increased momentum of technological enhancements in modeling and simulation, soon the digital human models will be able to interact with the material world, extending the horizons of virtual modeling and testing.

1.1 Problem definition and motivation

One of the major challenges facing current digital human modeling is ability to model and analyze equipment attached to the body. This challenge can be addressed by leveraging advances in the field of multibody system dynamics. Multibody system dynamics is based on classical and analytical mechanics, and the theories developed are applied to a wide variety of engineering systems such as interconnected mechanical systems, robotics and walking mechanisms.

The main purpose of this research is to develop a method to simulate the motion of attached equipment on the human body and its effect on the motion of the human body. To explain the problem further, consider the models shown in Figure 1-1(a), it shows the human body that is modeled as a linked mechanism. Figure 1-1 (b) shows the equipment that may be modeled as a spring-mass-damper system. Figure 1-1 (c) shows the human body with the attached equipment and its mechanical model. Thus the problem is to simulate motion of the combined system as the human performs various tasks.

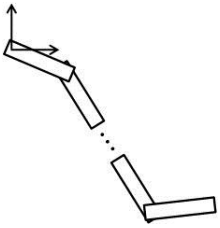

Real model Mechanical model

(a) Real and simplified mechanical model for the primary system

or

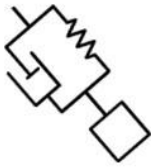

Real model Mechanical model

(b) Real and simplified mechanical model for the secondary system

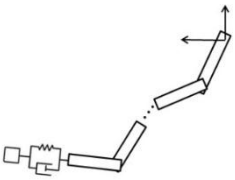

Real model Mechanical model

(c) Real and simplified model for the combined system

Figure 1-1 Equipment simulation – problem definition

1.2 Predictive dynamics approach for simulation of human motion

In general, forward dynamics and inverse dynamics are used to solve common mechanical problems. Forward dynamics solves for unknown response such as displacement, velocity and acceleration with known applied force. On the other hand, inverse dynamics solve for the unknown force by using equations of motion including known kinematic information. However, only limited information is available about kinematics and kinetics to solve a bio-system such as human motion. In this case, optimization-based predictive dynamics method is used to solve the problem. Figure 1-2 shows predictive dynamics flow chart.

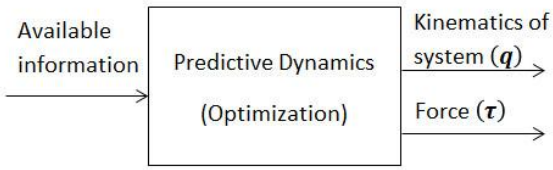

Figure 1-2 Predictive dynamics flow chart

1.3 Proposed approach

Figure 1-3 shows two basic approaches to solve the problem defined in Section 1.1. The first approach, shown in Figure 1-3 (a) is to re-derive the equations of motion for the combined skeletal and the equipment models and solve the resulting equations. The approach appears to be simple and straightforward. Existing multibody dynamics software can be used to solve the problem. The difficulty with this approach is that when a new equipment is attached to the body, the model needs to be updated and re-solved. In addition, the difficulty of integrating equations of motion with inequality constraints is

encountered. This difficulty was overcome with the predictive dynamics approach as explained earlier in Section 1.2.

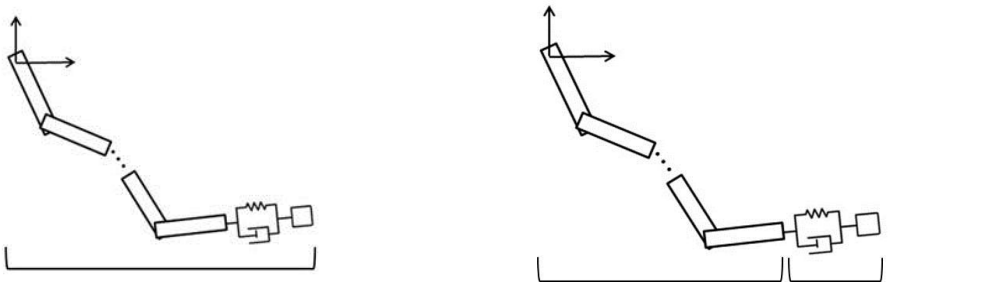

(a) Simulating the primary and secondary system as a single system

(b) Simulating the primary and secondary systems at two independent systems while accounting for the coupling motion, forces and moment

Figure 1-3 Two approaches to simulating the equipment interaction with the human body

In the proposed approach, shown in Figure 1-3(b), we divide the complete model into two subsystems, the primary system and the secondary system. The primary system consists of the skeletal model of the human body and the secondary system consists of the model for the equipment.

In the predictive dynamics approach, kinematic information of the attachment point on the primary system is available at each time. Based on the kinematic information and by solving equations of motion of the secondary system, reaction force and moment from secondary system are calculated. The calculated reaction force and moment affect motion of the primary system. Eventually, kinematic information of the attachment point of the primary system is updated due to the reaction force and moment. And then, the updated reaction force and moment are calculated from the secondary

system again. Therefore, at each time step, the updated kinematic information, reaction force and moment are calculated in the predictive dynamics optimization loop.

According to the introduced relationship between primary system and secondary system, this method is more modular and scalable to observe secondary system motion. As a result, the motion of the secondary system is easily observed no matter how many links the primary system has.

In this study, we develop methods that model the force interaction of the equipment and the human body using a simplified model of upper and lower arm with external equipment. First of all, one-link pendulum and the equipment which is modeled as a spring-mass-damper system attached to the primary system is analyzed and tested. The displacement, acceleration and reaction force are calculated and compared with the SimMechanics benchmarking solution. Moreover, the upper and lower arm is modeled as a two-link manipulator and the secondary system which is spring-mass-damper system attached to the two-links primary system. A spring-damper force perpendicular to the plane of collision is applied at all times whose direction depends on the motion of the equipment. The impact forces are collinear with the normal direction. By principle of interaction, these forces are of the same size but applied in opposite direction of the spring and damper forces. Such implementation avoids the need for modifying the existing validated kinematic and dynamic model of the primary system, either the two-link pendulum or the digital human model. The modularity also allows addition and removal of different equipment as needed without the need to re-derive the kinematic and dynamic equations.

The proposed method is tested on a simple case of a two degree of freedom serial chain mechanism with a simple passive system to behave as external equipment. In particular, the passive mass is assumed to be connected to the primary system by a spring and damper. The motion of the two-link manipulator was simulated using predictive dynamics module. This approach can be extended to a full-body 3D digital human model

and interaction of various equipment like helmet and backpack can be simulated as the digital human performs various tasks.

The proposed method is tested on a simple case of a two degree of freedom serial chain mechanism which is the called primary system with a simple passive system which is the secondary system to model the external equipment (Figure 1-4). In particular, the secondary system is assumed as the spring, damper and mass system which is attached to the primary system. The two-link pendulum problem is considered as human's lower and upper arm. To allow for simulation of digital human motion with multiple external equipment, the secondary system is modeled separately. This way a new secondary system can be treated easily.

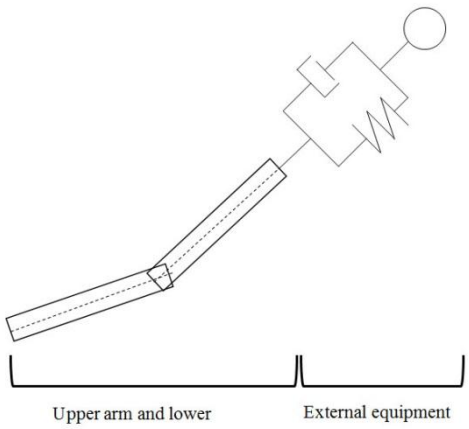

Figure 1-4 Modeling upper arm, lower arm and external equipment

1.4 Review of literature

Due to the complex mechanical behavior of the human body, the problem of inverse dynamics is not solvable in a trivial manner for impacts (Gruber *et al*, 1998). Also, parallel and vector computation are introduced in order to compute multibody

equations of motion in an adequate computer environment (Fisette *et al*, 1998). In other words, there is still interest on multibody systems in analytical and numerical mathematics resulting in reduction methods for rigorous treatment of simple models and special integration code for ODE (Ordinary Differential Equation) and DAE (Differential Algebraic Equations) representations supporting the numerical efficiency in biomechanics, robotics and vehicle dynamics (Schiehlen, 1997). Predictive dynamics is one such DAE solving algorithm applied to digital human modeling and simulation. It is an optimization-based methodology to predict physically-realistic human motions while avoiding integrating the typical differential algebraic equations. Instead, the methodology imposes the equations of motions as constraints in the optimization problem, thus allowing use of highly redundant and anatomically correct joint-based full-body human models with relatively less computational expense. The equations of motion for a class of dynamical systems, two-degree-of-freedom oscillators with cubic non-linearity in the restoring forces, were examined and showed coupling effect (Verros *et al*, 1999). Each task is characterized by an objective function and a unique set of constraints that define the task. The equations of motion are assembled in a canonical form rather than derived in terms of the total momentum of the system to gain numerical efficiency and stability (Lankarani *et al*, 2001). Various task motions have been predicted and validated using predictive dynamics approach with physics-based digital human model (Abdel-Malek *et al*, 2008). To ensure the realism and to get useful feedback from such digital human models, the interaction of the humans with the objects must respect the fundamental principles of mechanics. Researchers have tried to simulate 3D human motions using theories from mechanics and multibody dynamics. However, the work of the computational mechanics community focuses on an accurate description of interaction through a theoretical, experimental and numerical frame work. Such a focus on detail increases the complexity of models which leads to heavy computations (Renouf *et al*, 2005).

1.5 Overview of thesis

The rest of thesis is organized as follows. The dynamic models for the primary one-link system, the secondary mass-spring-damper system, and the combined system are developed in Chapter 2. These models are then analyzed to understand the reaction forces and moments applied on the primary system due to the presence of the secondary system. The dynamic models for the primary two-link system combined with the secondary mass-spring-damper system are developed in Chapter 3. In addition, the calculation of reaction force and moment are described and the validation of developed approach is shown. In Chapter 4, predictive dynamics algorithm is introduced. The algorithm is then modified to suit the new approach to simulating the equipment. The changes allow application of interaction forces on the primary two-link system due to the presence of the secondary spring-mass-damper system. This approach is implemented and the numerical results are presented in Chapter 5. The results are compared with a benchmark solution obtained by solving the full system using SimMechanics toolbox. Finally, the conclusions, discussion, and avenues for future work are presented in Chapter 6.

CHAPTER 2

ONE-LINK PRIMARY SYSTEM WITH SECONDARY SYSTEM

In this chapter, the idea of simulating a complex multi-body dynamics system as a combination of two independent systems, a primary and a secondary system, as introduced in Chapter 1 is implemented. A planar two degree-of-freedom (dof) system is chosen as a simple test case. In particular, a one-link simple pendulum is modeled as a primary system while a mass with spring-damper system is modeled as secondary system. The two systems would interact with each other by sharing the reaction forces and motion at the point of connection. We also develop a mathematical model for the full (two dof) system. The solution of this full system model would serve as the benchmark solution and the results from our approach will be compared against the results of full system model.

First of all, equations of motion of three different systems, a one dof one link system, one dof spring-mass-damper system with kinematic motion as input and a two dof system composed of one dof one link system with spring-mass-damper system, are derived by using Lagrange's Equation. The reaction forces and moments on the secondary system due to the motion of the primary system are then calculated. The components of the equations of motion of the two independent systems and the full two dof system are then compared. By comparing equations of motion of two approaches, force terms on the secondary system can be verified. In addition, free body diagrams on the secondary system mass and entire systems shows that reaction force and moment at the attachment point of secondary system.

2.1 One-link equation of motion

Consider a planar one dof simple pendulum with mass m_1 and link length L_1 as shown in Figure 2-1. The center of mass of the link is assumed to be located at half the link length. The Table 2-1 shows given data for the parameters.

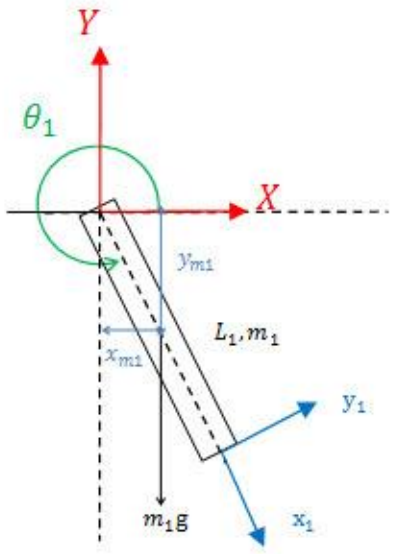

X, Y= Inertial reference frame

$x_{i,}\, y_i$ = *i*th local coordinate

L_1 = Length of 1st link

m_1 = Mass of 1st link

$x_{m1,}\, y_{m1}$ = Distance from inertial reference frame to center of mass of 1st link

θ_1 = Angle that the 1st link makes with inertial frame

g = Acceleration of gravity (m/s^2)

Figure 2-1 Model of planar one-link simple pendulum

Table 2-1 Data of planar one-link simple pendulum

L(m)	m_1(kg)	θ_1(rad)	g(m/s^2)
1.0	1.0	0.0	9.81

The equation of motion for one-link pendulum can be derived by using Lagrange's Equation. Assuming θ_1 to be generalized coordinate, the position of the center of the simple pendulum (x_{m1}, y_{m1}) and their derivative forms with respect to (w.r.t) time are

$$x_{m1} = \frac{L_1}{2}\cos\theta_1 \,, y_{m1} = \frac{L_1}{2}\sin\theta_1 \tag{2.1}$$

$$\dot{x}_{m1} = -\frac{L_1}{2}\dot{\theta}_1 \sin\theta_1 \,, \dot{y}_{m1} = \frac{L_1}{2}\dot{\theta}_1 \cos\theta_1 \tag{2.2}$$

The potential energy (V) is thus calculated as:

$$\mathrm{V} = \frac{m_1 g L_1}{2} \sin\theta_1 \tag{2.3}$$

and the kinetic energy (T) is obtained as:

$$\mathrm{T} = \frac{1}{2} m_1 ((\dot{x}_{m1})^2 + (\dot{y}_{m1})^2) = \frac{{L_1}^2 m_1}{8} \dot{\theta_1}^2 \tag{2.4}$$

The equation of motion can now be calculated using the Lagrange's Equation given as:

$$\frac{d}{dt}\left(\frac{\partial \mathrm{T}}{\partial \dot{q}}\right) - \frac{\partial T}{\partial q} + \frac{\partial V}{\partial q} + \frac{\partial R}{\partial \dot{q}} = 0$$

Where q is the generalized coordinate, $\dot{q}$ is the time derivative of the generalized coordinate, and *R* is Rayleigh dissipation function.

Substituting values from equations from the equation of motion w.r.t. θ_1 is obtained as:

$$I\ddot{\theta}_1 + \frac{m_1 g L_1}{2} \cos\theta_1 = 0 \quad \text{where } I = \frac{L_1^2 m_1}{4} \tag{2.5}$$

2.2 Spring-mass-damper with kinematic motion as input

Consider only one dof spring-mass-damper system with kinematic motion as input as shown in Figure 2-2. The kinematic information at each given time is obtained from primary system by using predictive dynamics module.

The secondary system is described in Figure 2-2 with kinematic information from primary system. The equations of motion of secondary system can be derived by using Lagrange's equation. The positions of the center of mass of secondary system (x_m, y_m) can be expressed as:

$$x_m = x + r\cos\theta_i\,,\ y_m = y + r\sin\theta_i \tag{2.6}$$

and their derivative forms w.r.t time are

$$\dot{x}_m = \dot{x} + \dot{r}\cos\theta_i - r\,\dot{\theta}_\iota \sin\theta_i \tag{2.7}$$

$$\dot{y}_m = \dot{y} + \dot{r}\sin\theta_i + r\,\dot{\theta}_\iota \cos\theta_i$$

The potential energy (V) of the system is calculated as:

$$V = mg(y + r\sin\theta_i) + \frac{1}{2}k(r - r_0)^2 \tag{2.8}$$

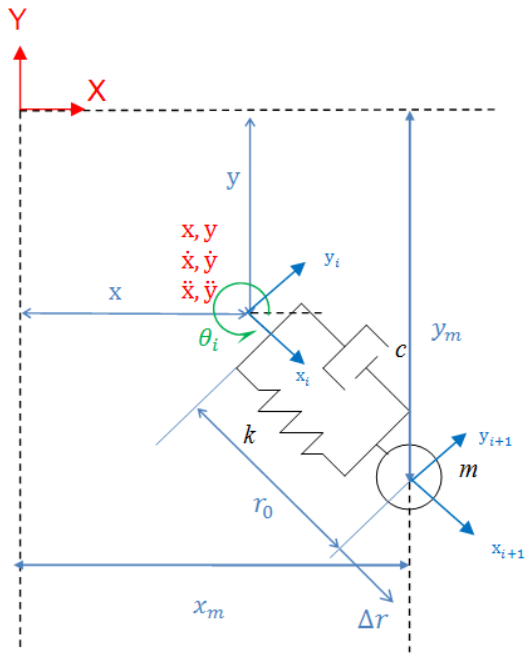

X, Y= Inertial reference frame

x_i, y_i = ith local coordinate

θ_i = Angle measured from i-1th frame

g = Acceleration of gravity

r_0 = Initial length of spring

Δr = Change of spring length

$r = r_0 + \Delta r$

c = Damping coefficient

k = Spring constant

m = Mass of secondary system

x_m, y_m = Distance from inertial reference frame to center of mass of secondary system (m)

Kinematic information of primary system

x, y = Distance from inertial reference frame to secondary system

ẋ, ẏ = Velocity to x,y direction

ẍ, ÿ = Acceleration to x,y direction

Figure 2-2 Spring-mass-damper system with kinematic motion as input

The kinetic energy (T) is obtained as:

$$T = \frac{1}{2}m((\dot{x}_m)^2 + (\dot{y}_m)^2) \tag{2.9}$$

$$= \frac{1}{2}m\left(\left(\dot{x} + \dot{r}\cos\theta_i - r\,\dot{\theta}_i \sin\theta_i\right)^2 + \left(\dot{y} + \dot{r}\sin\theta_i + r\,\dot{\theta}_i \cos\theta_i\right)^2\right) \tag{2.10}$$

$$= \frac{m\dot{x}^2}{2} + \frac{m\dot{y}^2}{2} + m\dot{r}\dot{x}\cos\theta_i + mr\dot{y}\dot{\theta}_i\cos\theta_i \tag{2.11}$$

$$+ \frac{m\dot{r}^2}{2} + \frac{mr^2\dot{\theta}_i^{\,2}}{2} + m\dot{r}\dot{y}\sin\theta_i - mr\dot{x}\dot{\theta}_i\sin\theta_i$$

Therefore, equation of motion w.r.t. r is calculated:

The equations of motion w.r.t the generalized coordinate r are given as

$$m\ddot{r} + c\dot{r} + \left(k - m\dot{\theta}_i^{\,2}\right) r = kr_0 - m\ddot{x}\ cos\,\theta_i - m(\mathrm{g} + \ddot{y})\,sin\,\theta_i \qquad (2.12)$$

2.3 Equation of motion of planar one-link simple pendulum with attached spring-mass-damper

Consider a one-link system with spring-mass-damper attached at the end of the link as shown in Figure 2-3.

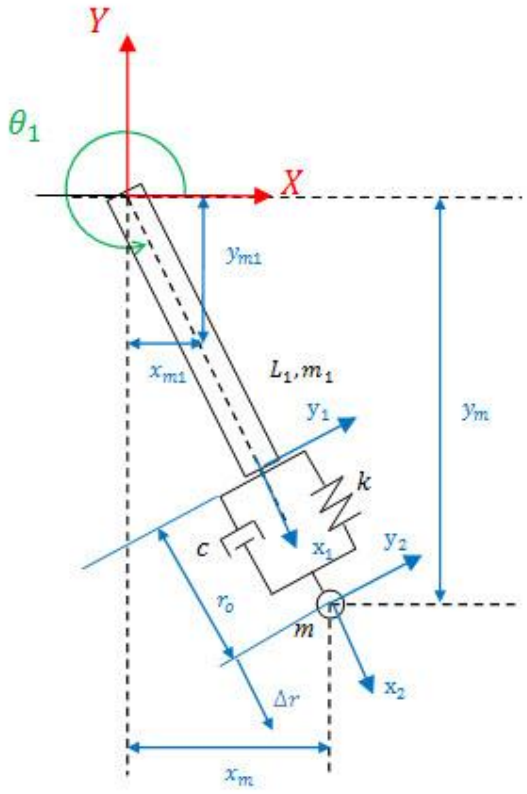

X, Y= Inertial reference frame

x_i, y_i = ith local coordinate

L_1 = Length of 1 link

m_1 = Mass of 1 link

x_{m1}, y_{m1} = Distance from inertial reference frame to center of mass of 1 link (m_1)

θ_1 = Angle that the simple pendulum makes with inertial frame

g = Acceleration of gravity ($\mathrm{m/s^2}$)

r_0 = Initial length of spring

Δr = Change of spring length

$r = r_0 + \Delta r$

c = Damping coefficient

k = Spring constant

m = Mass of ball

x_m, y_m = Distance from inertial reference frame to center of mass of ball (m)

Figure 2-3 Model of one-link simple pendulum with attached spring-mass-damper system

Table 2-2 Data of one-link simple pendulum with attached spring-mass-damper system

$L(\mathrm{m})$	$m_1(\mathrm{kg})$	$\theta_1(\mathrm{rad})$	$\mathrm{g}(\mathrm{m/s^2})$	$r_0(\mathrm{m})$	$c(\mathrm{N\cdot s/m})$	$k(\mathrm{N/m})$	m (kg)
1.0	1.0	0.0	9.81	0.0	30	1000	0.2

Similarly, the equations of motion for one-link pendulum with spring-mass-damper system can be derived by using Lagrange's Equation. For the system described in Figure 2-3, the generalized coordinates are θ_1 and r. The position of the center of the simple pendulum (x_{m1}, y_{m1}) and the center of mass of the ball (x_m, y_m) can be expressed as:

$$x_{m1} = \frac{L}{2}\cos\theta_1 \, , y_{m1} = \frac{L}{2}\sin\theta_1 \tag{2.13}$$

$$x_m = (L + r)\cos\theta_1 \, , y_m = (L + r)\sin\theta_1 \tag{2.14}$$

and their derivative forms w.r.t time are

$$\dot{x}_{m1} = -\frac{L}{2}\dot{\theta}_1 \sin\theta_1 \ \, , \dot{y}_{m1} = \frac{L}{2}\dot{\theta}_1 \cos\theta_1 \tag{2.15}$$

$$\dot{x}_m = \dot{r}\cos\theta_1 - (L + r)\dot{\theta}_1 \sin\theta_1 \ \, , \dot{y}_m = \dot{r}\sin\theta_1 + (L + r)\dot{\theta}_1 \cos\theta_1 \tag{2.16}$$

Similarly, potential energy (V) of the system is calculated as:

$$\mathrm{V} = m_1 \mathrm{g}\left(\frac{L}{2}\sin\theta_1\right) + mg\big((L + r)\sin\theta_1\big) + \frac{1}{2}k(r - r_0)^2 \tag{2.17}$$

and the kinetic energy (T) is shown as:

$$\mathrm{T} = \frac{1}{2}m_1((\dot{x}_{m1})^2 + (\dot{y}_{m1})^2) + \frac{1}{2}m((\dot{x}_m)^2 + (\dot{y}_m)^2) \tag{2.18}$$

$$= \frac{1}{8}\left(L^2 m_1 \dot{\theta}_1{}^2 + 4m\left(\dot{r}^2 + (L + r)^2 \dot{\theta}_1{}^2\right)\right)$$

Therefore, the Lagrange's Equation is:

$$\frac{d}{dt}\left(\frac{\partial \mathrm{T}}{\partial \dot{q}}\right) - \frac{\partial T}{\partial q} + \frac{\partial V}{\partial q} + \frac{\partial R}{\partial \dot{q}} = 0$$

Where q is the generalized coordinate, $\dot{q}$ is the time derivative of the generalized coordinate, and R is Rayleigh dissipation function.

The equation of motion w.r.t. θ_1 is obtained as:

$$\frac{1}{4}\left({L_1}^2(4m+m_1)+8L_1mr+4mr^2\right)\ddot{\theta}_1+2\,m(L_1+r)\dot{r}\dot{\theta}_1 \qquad (2.19)$$

$$=-\frac{1}{2}\mathrm{g}(L_1(2m+m_1)+2mr)\cos\theta_1$$

Finally, equation of motion w.r.t. r is obtained with similar way.

$$m\ddot{r}+c\dot{r}+\left(k-m{\dot{\theta}_1}^2\right)r=mL_1{\dot{\theta}_1}^2-mg\,\sin\theta_1+kr_0 \qquad (2.20)$$

2.4 Analysis of two different systems with new approach

It is assumed that $m=0$ and $r=0$ in Eq. (2.19) which is equation of motion for one-link pendulum with spring-mass-damper system w.r.t. θ. Then the equation of motion is simplified and exactly matches with Eq. (2.5) which is equation of motion for one-link pendulum.

If Eq. (2.19) is expanded and observed

$$\frac{L^2m_1}{4}\ddot{\theta}_1+\frac{m_1gL}{2}\cos\theta_1+(L+r)^2m\ddot{\theta}_1+2m(L+r)\dot{r}\dot{\theta}_1+gm(L+r)\cos\theta_1=0 \qquad (2.21)$$

The first two terms are the same with equation of motion of the simple pendulum so that the rest of terms are from secondary system. Based on these terms and Eq. (2.5), additional forces on the ball can be calculated.

$$a_{\theta_1}=(L+r)\ddot{\theta}_1+2\dot{r}\dot{\theta}_1 \qquad (2.22)$$

$$F_{\theta_1}=\left[(L+r)\ddot{\theta}_1+2\dot{r}\dot{\theta}_1\right]m \qquad (2.23)$$

$$M=\left[(L+r)\ddot{\theta}_1+2\dot{r}\dot{\theta}_1\right](L+r)m+gm(L+r)\cos\theta_1 \qquad (2.24)$$

Eq. (2.23) shows force in θ_1 direction based on Eq. (2.22) and Eq. (2.24) is moment equation of only secondary system mass (m). Actually, the third, fourth and fifth terms of Eq. (2.21) are the same with moment form of secondary system mass which is Eq. (2.24).

Similarly, Eq. (2.25) provides acceleration equation in r direction so that force F_r is calculated by Eq. (2.26).

$$a_r = \ddot{r} - (L + r)\dot{\theta_1}^2 \tag{2.25}$$

$$F_r = m\ddot{r} - m(L + r)\dot{\theta_1}^2 \tag{2.26}$$

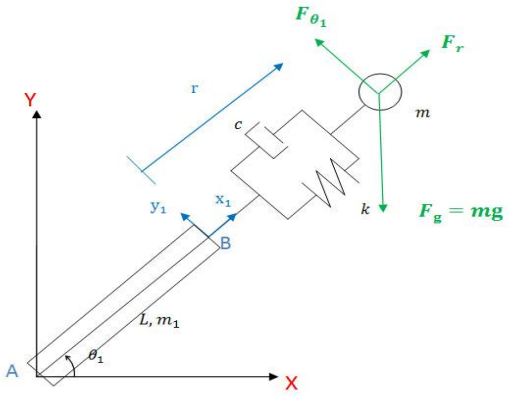

Figure 2-4 Forces on the secondary system mass

The equations of motion for one-link pendulum with spring-mass-damper system can be verified by establishing equations of equilibrium at each system with calculated forces and moment. First, free body diagram and equation of equilibrium for mass of the secondary system are checked.

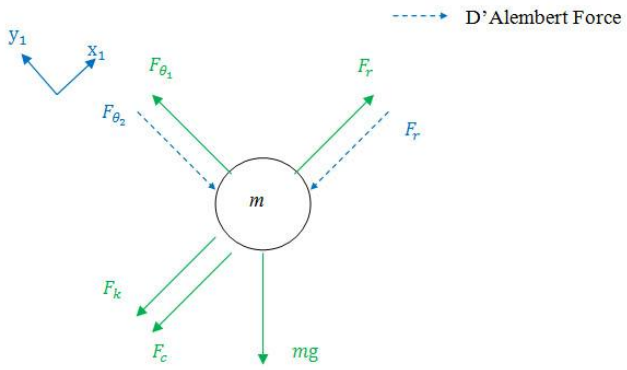

Figure 2-5 Free body diagram at secondary system mass

$$+\nearrow \sum \mathrm{x}_1 = 0 \tag{2.27}$$

$$-\mathrm{F}_r - F_k - F_c - mg\sin\theta_1 = 0 \tag{2.28}$$

where F_k is spring force.

F_c is damper force.

F_r is substituted from Eq. (2.26) and the rearranged Eq. (2.28) becomes

$$m\ddot{r} + c\dot{r} + \left(k - m\dot{\theta_1}^2\right)r = mL\dot{\theta_1}^2 - mg\sin\theta_1 + kr_0 \tag{2.29}$$

$$m\ddot{r} + c\dot{r} + kr = m\dot{\theta_1}^2(L + r) - mg\sin\theta_1 + kr_0 \tag{2.30}$$

Equation. (2.29) is well matched with equation of motion for one-link pendulum with spring-mass-damper w.r.t r which is already derived in Eq. (2.20). Also, Eq. (2.28) can expressed as

$$\mathrm{F}_r + mg\sin\theta_1 = -\mathrm{F}_k - \mathrm{F}_c \tag{2.31}$$

where $\mathrm{F}_r = m\ddot{r} - m\dot{\theta_1}^2(L + r)$

$$\mathrm{F}_c = -c\dot{r}$$

$$\mathrm{F}_k = -k(r - r_0)$$

Similarly, free body diagram and equation of equilibrium for primary and secondary system are checked.

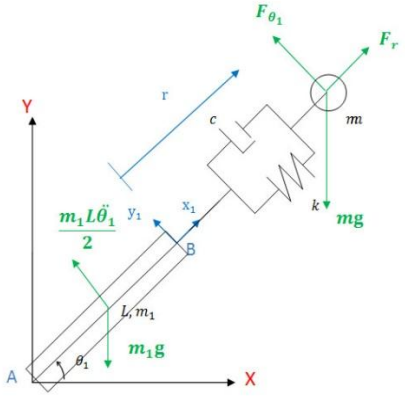

Figure 2-6 Free body diagram of one-link pendulum with spring-mass-damper system

$$+\circlearrowleft \sum \mathrm{M_A} = 0 \tag{2.32}$$

$$-\frac{L^2 m_1}{4}\ddot{\theta_1} - \mathrm{F}_{\theta_1}(L+r) - (mg\cos\theta_1)(L+r) - (m_1 g\cos\theta_1)\frac{L}{2} = 0 \tag{2.33}$$

F_θ is substituted from Eq. (2.23) and the rearranged Eq. (2.33) becomes

$$\frac{L^2 m_1}{4}\ddot{\theta_1} + (L+r)^2 m\ddot{\theta_1} + 2m(L+r)\dot{r}\dot{\theta_1} + mg\cos\theta_1\,(L+r) + m_1 g\cos\theta_1\frac{L}{2} = 0 \tag{2.34}$$

It is also easily checked that Eq. (2.34) is the same as Eq. (2.19) which is equation of motion for simple pendulum with spring-mass-damper w.r.t θ_1

CHAPTER 3

TWO-LINK PRIMARY SYSTEM WITH SECONDARY SYSTEM

In this chapter, primary system is extended to two-link simple pendulum instead of one-link simple pendulum. Basically, the equations of motion of two-link simple pendulum with secondary system are derived by Lagrange's equation. They are compared with equations of motion of two-link simple pendulum so that forces on the secondary system are analyzed.

Section 3.1 derives equation of motion of two-link simple pendulum with spring-mass-damper system. In Section 3.2, reaction forces and moment are calculated and changed to global force form. Section 3.3 is about validation of the proposed approach. Since it is assumed that the primary system and secondary system are solved separately, there are two approaches to solve the systems before the two systems are solved with interacting forces and moment. First, solution of the secondary system with known primary system motion is shown in Section 3.4. The solution of the primary system with known secondary system motion is explained in Section 3.5

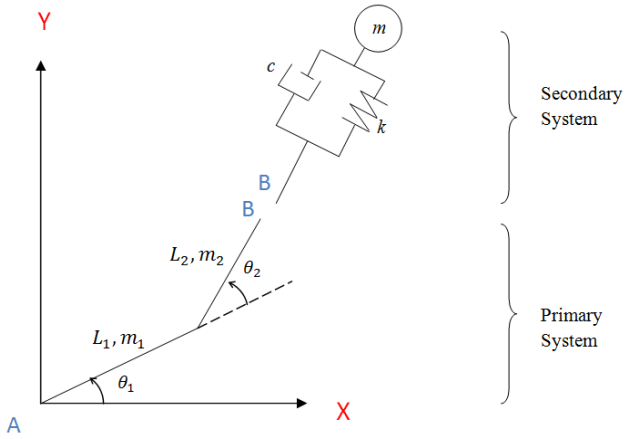

Figure 3-1 Planar two dof pirmary system and one dof secondary system

3.1 Equation of motion of two-link simple pendulum with spring mass damper

In this section, the governing equations for a two-link primary system with one dof spring-mass-damper secondary system are developed to verify motions of the system and to understand the interaction forces and moment between the two systems. Consider the system described in Figure 3-2 with two links of length L_1 and L_2 and mass m_1 and m_2, such that the center of mass is located at the center of each link. The corresponding data for simulation is provided in Table 3-1.

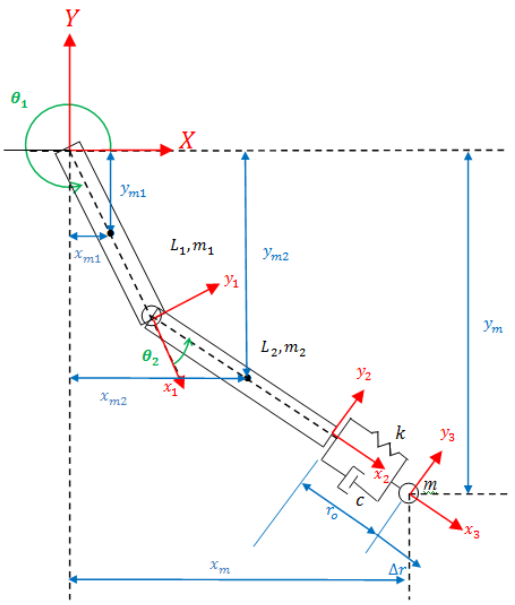

X, Y= Inertial reference frame

x_i, y_i = ith local coordinate

L_i = Length of ith link

m_i = Mass of ith link

x_{mi}, y_{mi} = Distance from inertial reference frame to center of mass of ith link

θ_i = Angle measured from i-1th frame

g = Acceleration of gravity

r_0 = Initial length of spring

Δr = Change of spring length

$r = r_0 + \Delta r$

c = Damping coefficient

k = Spring constant

m = Mass of secondary system

x_m, y_m = Distance from inertial reference frame to center of mass of secondary system (m)

Figure 3-2 Two-link simple pendulum with spring-mass-damper system

Table 3-1 Data of two-link simple pendulum with spring-mass-damper system

L_1(m)	m_1(kg)	L_2(m)	m_2(kg)	m(kg)	θ_1(rad)
1.2	1.2	0.9	0.8	0.2	$-\frac{\pi}{4}$
θ_2(rad)	g(m/s^2)	r_0(m)	c(N · s/m)	k(N/m)	
0.0	9.81	0.0	30	1000	

The equations of motion for two-link pendulum with spring-mass-damper system can be derived by using Lagrange's equation. For the system described in Figure 3-2, the generalized coordinates are θ_1, θ_2 and r. The positions of the center of mass of the two-link pendulum (x_{m1}, y_{m1}) and (x_{m2}, y_{m2}) and the center of mass of secondary system (x_m, y_m) can be expressed as:

$$x_{m1} = \frac{L_1}{2}\cos\theta_1 \,, y_{m1} = \frac{L_1}{2}\sin\theta_1$$

$$x_{m2} = L_1\cos\theta_1 + \frac{L_2}{2}\cos(\theta_1+\theta_2)$$

$$y_{m2} = L_1\sin\theta_1 + \frac{L_2}{2}\sin(\theta_1+\theta_2) \qquad (3.1)$$

$$x_m = L_1\cos\theta_1 + (L_2+r)\cos(\theta_1+\theta_2)$$

$$y_m = L_1\sin\theta_1 + (L_2+r)\sin(\theta_1+\theta_2)$$

and their derivative forms w.r.t time are

$$\dot{x}_{m1} = -\frac{L_1}{2}\dot{\theta}_1\sin\theta_1$$

$$\dot{y}_{m1} = \frac{L_1}{2}\dot{\theta}_1\cos\theta_1$$

$$\dot{x}_{m2} = -L_1\dot{\theta}_1\sin\theta_1 - \frac{L_2}{2}\sin(\theta_1+\theta_2)\left(\dot{\theta}_1+\dot{\theta}_2\right) \qquad (3.2)$$

$$\dot{y}_{m2} = L_1\dot{\theta}_1\cos\theta_1 + \frac{L_2}{2}\cos(\theta_1+\theta_2)\left(\dot{\theta}_1+\dot{\theta}_2\right)$$

$$\dot{x}_m = -L_1\dot{\theta}_1\sin\theta_1 + \dot{r}\cos(\theta_1+\theta_2) - (L_2+r)\sin(\theta_1+\theta_2)\left(\dot{\theta}_1+\dot{\theta}_2\right)$$

$$\dot{y}_m = L_1\dot{\theta}_1 \cos\theta_1 + \dot{r}\sin(\theta_1+\theta_2) + (L_2+r)\cos(\theta_1+\theta_2)\left(\dot{\theta}_1+\dot{\theta}_2\right)$$

The potential energy (V) of the system is calculated as:

$$\begin{aligned} \mathrm{V} &= m_1 g y_{m1} + m_2 g y_{m2} + m g y_m + \tfrac{1}{2}k(r-r_0)^2 \\ &= m_1 g\left(\tfrac{L_1}{2}\sin\theta_1\right) + m_2 g\left(L_1\sin\theta_1 + \tfrac{L_2}{2}\sin(\theta_1+\theta_2)\right) \\ &+ m g(L_1\sin\theta_1 + (L_2+r)\sin(\theta_1+\theta_2)) + \tfrac{1}{2}k(r-r_0)^2 \end{aligned} \tag{3.3}$$

And the kinetic energy (T) is obtained as:

$$\begin{aligned} \mathrm{T} &= \tfrac{1}{2}m_1((\dot{x}_{m1})^2 + (\dot{y}_{m1})^2) + \tfrac{1}{2}I_{c1}\dot{\theta}_1^{\,2} \\ &+ \tfrac{1}{2}m_2((\dot{x}_{m2})^2 + (\dot{y}_{m2})^2) + \tfrac{1}{2}I_{c2}\left(\dot{\theta}_1+\dot{\theta}_2\right)^2 \\ &+ \tfrac{1}{2}m((\dot{x}_m)^2 + (\dot{y}_m)^2) \end{aligned} \tag{3.4}$$

where $I_{c1} = \frac{m_1 {L_1}^2}{12}$ and $I_{c2} = \frac{m_2 {L_2}^2}{12}$

The equation of motion can be now obtained using the Lagrange's equation, given as:

$$\frac{d}{dt}\left(\frac{\partial \mathrm{T}}{\partial \dot{q}}\right) - \frac{\partial T}{\partial q} + \frac{\partial V}{\partial q} + \frac{\partial R}{\partial \dot{q}} = 0$$

where q is the generalized coordinate, $\dot{q}$ is the time derivative of the generalized coordinate, and R is Rayleigh dissipation function.

The three equations of motion w.r.t. θ_1, θ_2 and r are shown below:

$$\begin{aligned} &\left[\begin{matrix} L_2^2 m + \frac{L_2^2 m_2}{3} + L_1^2\left(m + \frac{m_1}{3} + m_2\right) + 2L_2 mr + mr^2 \\ + L_1\{L_2(2m+m_2) + 2mr\}\cos\theta_2 \end{matrix}\right]\ddot{\theta}_1 \\ &+\left[L_2^2\left(m+\frac{m_2}{3}\right) + 2L_2 mr + mr^2 + \frac{L_1}{2}\{L_2(2m+m_2)+2mr\}\cos\theta_2\right]\ddot{\theta}_2 \\ &+[L_1 m\sin\theta_2]\ddot{r} + \frac{1}{2}\left[\begin{matrix} \mathrm{g}L_1(m_1+2m_2)\cos\theta_1 \\ + L_2 m_2\{\mathrm{g}\cos(\theta_1+\theta_2) - L_1\dot{\theta}_2\left(2\dot{\theta}_1+\dot{\theta}_2\right)\sin\theta_2\} \end{matrix}\right] \\ &+ m\left[\begin{matrix} 2L_2\dot{r}\dot{\theta}_1 + 2L_2\dot{r}\dot{\theta}_2 + \mathrm{g}L_1\cos\theta_1 + 2L_1\dot{r}\dot{\theta}_1\cos\theta_2 + 2L_1\dot{r}\dot{\theta}_2\cos\theta_2 \\ + \mathrm{g}L_2\cos(\theta_1+\theta_2) - 2L_1L_2\dot{\theta}_1\dot{\theta}_2\sin\theta_2 - L_1L_2\dot{\theta}_2^2\sin\theta_2 \\ + r\{2\dot{r}\dot{\theta}_1 + 2\dot{r}\dot{\theta}_2 + \mathrm{g}\cos(\theta_1+\theta_2) - 2L_1\dot{\theta}_1\dot{\theta}_2\sin\theta_2 - L_1\dot{\theta}_2^2\sin\theta_2\} \end{matrix}\right] = 0 \end{aligned} \tag{3.5}$$

$$\left[L_2^2\left(m+\frac{m_2}{3}\right)+2L_2mr+mr^2+\frac{L_1}{2}\{L_2(2m+m_2)+2mr\}\cos\theta_2\right]\ddot{\theta}_1$$

$$+\left[L_2^2m+\frac{L_2^2m_2}{3}+2L_2mr+mr^2\right]\ddot{\theta}_2+\frac{1}{2}gL_2m_2\cos(\theta_1+\theta_2)$$

$$+\frac{1}{2}L_1L_2m_2\dot{\theta}_1^2\sin\theta_2 \qquad (3.6)$$

$$+m\begin{bmatrix}2L_2\dot{r}\dot{\theta}_1+2L_2\dot{r}\dot{\theta}_2+gL_2\cos(\theta_1+\theta_2)\\+L_1L_2\dot{\theta}_1^2\sin\theta_2+r\{2\dot{r}\dot{\theta}_1+2\dot{r}\dot{\theta}_2+g\cos(\theta_1+\theta_2)+L_1\dot{\theta}_1^2\sin\theta_2\}\end{bmatrix}=0$$

$$m\ddot{r}+c\dot{r}+k\Delta r+L_1m\sin\theta_2\,\ddot{\theta}_1 \qquad (3.7)$$

$$-m\left\{(L_2+r)\left(\dot{\theta}_1+\dot{\theta}_2\right)^2+L_1\dot{\theta}_1^2\cos\theta_2-g\sin\left(\dot{\theta}_1+\dot{\theta}_2\right)\right\}=0$$

If it is assumed that $m=0$ and $r=0$ in the equation of motion (Eq. (3.5)), it reduces to the governing equation of the two link system. Thus, the terms with m and r are the terms due to the presence of the secondary system. Some of these terms come from the motion of the secondary system, while others come due to the coupling effect.

3.2 Calculation of reaction forces and moment

The coupling terms added to the governing equations are derived in this section using an analytical approach. Based on free body diagram shown in Figure 3-3, three different forces exist on the secondary mass. By calculating accelerations of the attached mass in normal (x_{m2}) and tangential (y_{m2}) directions, the forces F_r and F_θ can be calculated as:

$$\begin{bmatrix}X_m\\Y_m\end{bmatrix}=\begin{bmatrix}\cos\theta_1&-\sin\theta_1\\\sin\theta_1&\cos\theta_1\end{bmatrix}\begin{bmatrix}L_1\\0\end{bmatrix}+\begin{bmatrix}\cos(\theta_1+\theta_2)&-\sin(\theta_1+\theta_2)\\\sin(\theta_1+\theta_2)&\cos(\theta_1+\theta_2)\end{bmatrix}\begin{bmatrix}L_2+r\\0\end{bmatrix} \qquad (3.8)$$

$$\begin{bmatrix}\dot{X}_m\\\dot{Y}_m\end{bmatrix}=\begin{bmatrix}\cos(\theta_1+\theta_2)\,\dot{r}-L_1\sin\theta_1\,\dot{\theta}_1-(L_2+r)\sin(\theta_1+\theta_2)\left(\dot{\theta}_1+\dot{\theta}_2\right)\\\sin(\theta_1+\theta_2)\,\dot{r}+L_1\cos\theta_1\,\dot{\theta}_1+(L_2+r)\cos(\theta_1+\theta_2)\left(\dot{\theta}_1+\dot{\theta}_2\right)\end{bmatrix} \qquad (3.9)$$

$$\begin{bmatrix}\ddot{x}_m\\\ddot{y}_m\end{bmatrix}=\begin{bmatrix}a_r\\a_\theta\end{bmatrix}=\begin{bmatrix}\cos(\theta_1+\theta_2)&\sin(\theta_1+\theta_2)\\-\sin(\theta_1+\theta_2)&\cos(\theta_1+\theta_2)\end{bmatrix}\begin{bmatrix}\ddot{X}_m\\\ddot{Y}_m\end{bmatrix} \qquad (3.10)$$

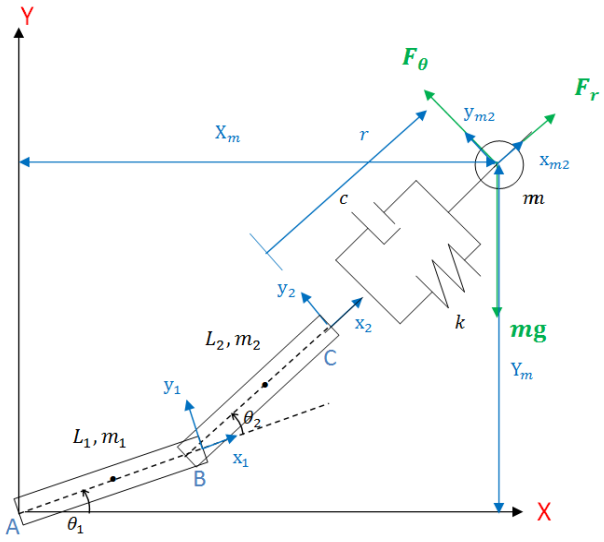

Figure 3-3 Two-link pendulum with spring-mass-damper system

$$= \begin{bmatrix} -L_2\dot{\theta}_1^2 - L_1\cos\theta_2\,\dot{\theta}_1^2 - r\dot{\theta}_1^2 - 2L_2\dot{\theta}_1\dot{\theta}_2 \\ -2r\dot{\theta}_1\dot{\theta}_2 - L_2\dot{\theta}_2^2 - r\dot{\theta}_2^2 + \ddot{r} + L_1\sin\theta_2\ddot{\theta}_1 \\ \cdots\cdots\cdots\cdots\cdots\cdots\cdots\cdots\cdots\cdots\cdots\cdots\cdots\cdots\cdots\cdots\cdots\cdots\cdots\cdots\cdots\cdots\cdots\cdots \\ 2\dot{r}\dot{\theta}_1 + L_1\sin\theta_2\,\dot{\theta}_1^2 + 2\dot{r}\dot{\theta}_2 + L_2\ddot{\theta}_1 \\ +L_1\cos\theta_2\,\ddot{\theta}_1 + r\ddot{\theta}_1 + L_2\ddot{\theta}_2 + r\ddot{\theta}_2 \end{bmatrix}$$

Therefore,

$$F_r = ma_r \tag{3.11}$$

$$F_\theta = ma_\theta \tag{3.12}$$

It is assumed that primary system and the secondary system are independent and reaction forces and moment are applied form the secondary system to primary system. The Point B in Figure 3-4 is the attachment point between two systems. These forces on the mass of secondary system are transmitted to the primary system at each instant. In order to observe interaction forces and moment between the two systems, the free body diagrams are drawn for secondary system and primary system.

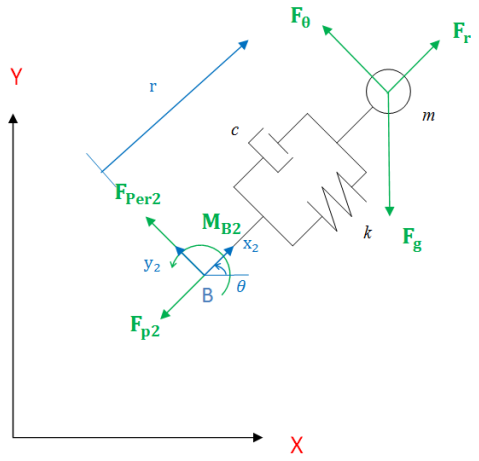

Figure 3-4 Free body diagram of secondary system

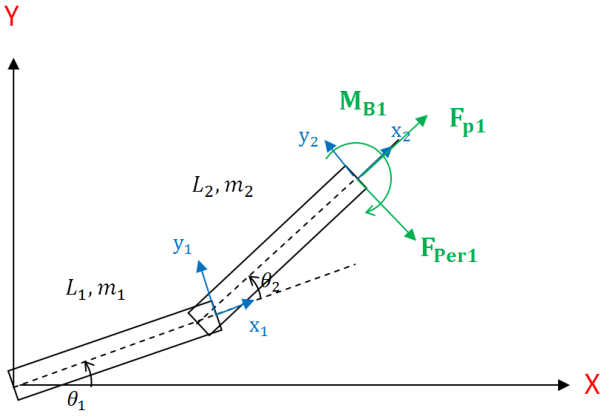

Figure 3-5 Free body diagram of primary system

Reaction forces F_{per} and F_{p} and moment M_{B} can be calculated such as:

$$\sum F_{y_2} = 0 \tag{3.13}$$

$$F_{\text{per2}} - F_\theta + F_g \sin\left(\frac{3\pi}{2} - \theta\right) = 0$$

where $\theta = \theta_1 + \theta_2$

$$F_{\text{per2}} = F_\theta - F_{\text{g}} \sin\left(\frac{3\pi}{2} - \theta\right) = -F_{\text{per1}}$$

$$\sum F_{\text{x}_2} = 0 \tag{3.14}$$

$$-F_{\text{p2}} - F_r + F_{\text{g}}\cos(\frac{3\pi}{2} - \theta) = 0$$

$$F_{\text{p2}} = -F_r + F_{\text{g}} \cos\left(\frac{3\pi}{2} - \theta\right) = -F_{\text{p1}}$$

$$\sum M_{\text{B2}} = 0 \tag{3.15}$$

$$M_{\text{B2}} - F_{\text{g}} r \cos\theta - F_\theta r = 0$$

$$M_{\text{B2}} = F_{\text{g}} r \cos\theta + F_\theta r = -M_{\text{B1}}$$

When solving the equations of motion for the primary system, these interaction forces should be applied to account for the reaction forces acting due to the presence of the secondary system. Therefore, equations of motion of two-link pendulum with reaction forces and moment can be expressed like

$$\frac{d}{dt}\left(\frac{\partial \text{T}}{\partial \dot{\theta}_1}\right) - \frac{\partial T}{\partial \theta_1} + \frac{\partial V}{\partial \theta_1} = Q_1 + M_{B1} \tag{3.16}$$

$$\frac{d}{dt}\left(\frac{\partial \text{T}}{\partial \dot{\theta}_2}\right) - \frac{\partial T}{\partial \theta_2} + \frac{\partial V}{\partial \theta_2} = Q_2 + M_{B1} \tag{3.17}$$

where $Q_1 = \mathbf{F}^{\text{T}} \cdot \frac{\partial r_p}{\partial \theta_1}$, $Q_2 = \mathbf{F}^{\text{T}} \cdot \frac{\partial r_p}{\partial \theta_2}$

Q_1 and Q_2 are generalized forces

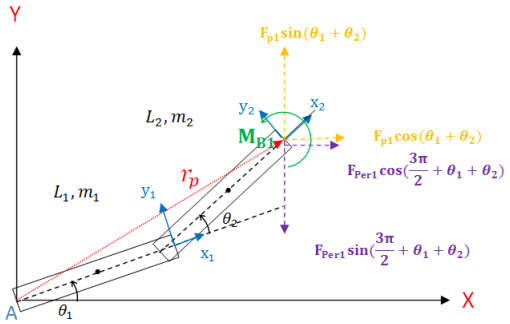

Figure 3-6 Free body diagram of primary system with forces and moment

We can derive **F** which is sum of decomposed reaction forces shown in Figure 3-6.

$$\mathbf{F} = \begin{bmatrix} F_{\text{per1}}\cos\left(\frac{3\pi}{2}+\theta_1+\theta_2\right) + F_{\text{p1}}\cos(\theta_1+\theta_2) \\ F_{\text{per1}}\sin\left(\frac{3\pi}{2}+\theta_1+\theta_2\right) + F_{\text{p1}}\sin(\theta_1+\theta_2) \end{bmatrix} \tag{3.18}$$

In addition, r_p is expressed such as

$$r_p = \begin{bmatrix} L_1\cos\theta_1 + L_2\cos(\theta_1+\theta_2) \\ L_1\sin\theta_1 + L_2\sin(\theta_1+\theta_2) \end{bmatrix} \tag{3.19}$$

And its derivatives w.r.t θ_1 and θ_2 are like

$$\frac{\partial r_p}{\partial \theta_1} = \begin{bmatrix} -L_1\sin\theta_1 - L_2\sin(\theta_1+\theta_2) \\ L_1\cos\theta_1 + L_2\cos(\theta_1+\theta_2) \end{bmatrix} \tag{3.20}$$

$$\frac{\partial r_p}{\partial \theta_2} = \begin{bmatrix} -L_2\sin(\theta_1+\theta_2) \\ L_2\cos(\theta_1+\theta_2) \end{bmatrix} \tag{3.21}$$

Therefore, we can calculate generalized forces Q_1 and Q_2 such as

$$Q_1 = \mathbf{F}^{\mathbf{T}}\frac{\partial r_p}{\partial \theta_1} \tag{3.22}$$

$$= -\left[F_{\text{per1}}\cos\left(\frac{3\pi}{2}+\theta_1+\theta_2\right) + F_{\text{p1}}\cos(\theta_1+\theta_2)\right][L_1\sin\theta_1 + L_2\sin(\theta_1+\theta_2)]$$

$$+[L_1\cos\theta_1 + L_2\cos(\theta_1+\theta_2)]\left[F_{p1}\sin(\theta_1+\theta_2) + F_{\text{per1}}\sin\left(\frac{3\pi}{2}+\theta_1+\theta_2\right)\right]$$

$$Q_2 = \mathbf{F}^{\mathbf{T}}\frac{\partial r_p}{\partial \theta_2} \tag{3.23}$$

$$= F_{\text{per1}}L_2\left[-\cos\left(\frac{3\pi}{2}+\theta_1+\theta_2\right)\sin(\theta_1+\theta_2) + \cos(\theta_1+\theta_2)\sin\left(\frac{3\pi}{2}+\theta_1+\theta_2\right)\right]$$

Therefore, the full equation of Eq. (3.16) and Eq. (3.17) are expresses like:

$$\left[\frac{L_1^2 m_1}{3} + L_1^2 m_2 + \frac{L_2^2 m_2}{3} + L_1 L_2 m_2\cos\theta_2\right]\ddot{\theta}_1 + \left[\frac{L_2^2 m_2}{3} + \frac{1}{2}L_1 L_2 m_2\cos\theta_2\right]\ddot{\theta}_2$$

$$+\frac{1}{2}gL_1 m_1\cos\theta_1 + gL_1 m_2\cos\theta_1 + \frac{1}{2}gL_2 m_2\cos(\theta_1+\theta_2)$$

$$-L_1 L_2 m_2\dot{\theta}_1\dot{\theta}_2\sin\theta_2 - \frac{1}{2}L_1 L_2 m_2\dot{\theta}_2^2\sin\theta_2 = \tag{3.24}$$

$$-\left[F_{\text{per1}}\cos\left(\frac{3\pi}{2}+\theta_1+\theta_2\right) + F_{\text{p1}}\cos(\theta_1+\theta_2)\right][L_1\sin\theta_1 + L_2\sin(\theta_1+\theta_2)]$$

$$+[L_1\cos\theta_1 + L_2\cos(\theta_1+\theta_2)]\left[F_{p1}\sin(\theta_1+\theta_2) + F_{\text{per1}}\sin\left(\frac{3\pi}{2}+\theta_1+\theta_2\right)\right]$$

$$-F_g r\cos\theta - F_\theta r$$

and

$$\left[\frac{L_2^2 m_2}{3} + \frac{1}{2}L_1 L_2 m_2\cos\theta_2\right]\ddot{\theta}_1 + \left[\frac{L_2^2 m_2}{3}\right]\ddot{\theta}_2$$

$$+\frac{1}{2}gL_2 m_2\cos(\theta_1+\theta_2) + \frac{1}{2}L_1 L_2 m_2\dot{\theta}_1^2\sin\theta_2 \qquad (3.25)$$

$$= F_{per1}L_2\left[-\cos\left(\frac{3\pi}{2}+\theta_1+\theta_2\right)\sin(\theta_1+\theta_2) + \cos(\theta_1+\theta_2)\sin\left(\frac{3\pi}{2}+\theta_1+\theta_2\right)\right]$$

$$-F_g r\cos\theta - F_\theta r$$

where $F_{per1} = -F_\theta + F_g\sin\left(\frac{3\pi}{2}-\theta\right)$

$$F_{p1} = F_r - F_g\cos\left(\frac{3\pi}{2}-\theta\right)$$

$$F_r = ma_r$$

$$F_\theta = ma_\theta$$

$$F_g = mg$$

3.3 Validation of current approach

The derivations and understanding obtained above for the new approach should be validated. To summarize, the approach involves two steps: First, simulating the primary system independently while considering the effect of interaction forces as external forces applied to the primary system. Second, these interaction forces are obtained by solving the motion of the secondary system, obtaining the state of the system at each time, and subsequently, calculating the forces and moments at the point of attachment to the primary system. In the next two sections, these two steps are validated.

3.4 Solution of secondary system with known primary system motion

In this section, it is assumed that the motion of the primary system is known when the secondary system is attached to the primary system. However, the motion of the

secondary system is unknown. The motion of the full system is solved by using MATLAB/SimMechanics. The solution for the primary system, $\boldsymbol{\theta_1}(\theta_1, \dot{\theta}_1$ and $\ddot{\theta}_1)$ and $\boldsymbol{\theta_2}(\theta_2, \dot{\theta}_2$ and $\ddot{\theta}_2)$, is used as known solution. Then, using the derived governing equations, the solution for the secondary system is obtained. When the governing equation is solved and the output is the motion of secondary system $\boldsymbol{r}$ $(r, \dot{r}$ and $\ddot{r})$. This solution is compared with the solution of the secondary system obtained benchmark solution $\boldsymbol{r}$ from MATLAB/SimMechanics. While there is continuous exchange of forces between primary and secondary system, the new approach will have discrete time intervals when the interaction would be considered. This test would allow us to understand the effect of time step size on the accuracy of the solution. The governing equation of the secondary system is:

$$m\ddot{r} + c\dot{r} + k\Delta r + L_1 m \sin\theta_2\, \ddot{\theta}_1 \tag{3.26}$$
$$-m\left\{(L_2 + r)\left(\dot{\theta}_1 + \dot{\theta}_2\right)^2 + L_1\dot{\theta}_1^2 \cos\theta_2 - \mathrm{g}\sin\left(\dot{\theta}_1 + \dot{\theta}_2\right)\right\} = 0$$

Rearranging the above equation and grouping the terms for different derivatives of the spring displacement r,

$$m\ddot{r} + c\dot{r} + \left[k - m\left(\dot{\theta}_1 + \dot{\theta}_2\right)^2\right] r \tag{3.27}$$
$$= L_2 m\dot{\theta}_1^2 + 2L_2 m\dot{\theta}_1\dot{\theta}_2 + L_2 m\dot{\theta}_2^2 + L_1 m\dot{\theta}_1^2\cos\theta_2$$
$$-L_1 m\ddot{\theta}_1\sin\theta_2 - mg\sin\left(\dot{\theta}_1 + \dot{\theta}_2\right) + kr_0$$

The Eq. (3.27) is simplified like

$$m\ddot{r} + c\dot{r} + \bar{k}_i r = F_i \tag{3.28}$$

$$\text{where } \bar{k}_i = k - m\left(\dot{\theta}_{1i} + \dot{\theta}_{2i}\right)^2$$

$$F_i = L_2 m\dot{\theta}_{1i}^2 + 2L_2 m\dot{\theta}_{1i}\dot{\theta}_{2i} + L_2 m\dot{\theta}_{2i}^2 + L_1 m\dot{\theta}_{1i}^2\cos\theta_{2i} \tag{3.29}$$
$$-L_1 m\ddot{\theta}_{1i}\sin\theta_{2i} - mg\sin(\theta_{1i} + \theta_{2i}) + kr_0$$

where i is time output.

If $\boldsymbol{\theta_1}$ and $\boldsymbol{\theta_2}$ are known, then the term on the RHS, F_i, is a constant that can be evaluated at each time instant. Thus a non-zero RHS of Eq. (3.28) makes it a nonhomogeneous ODE problem.

First of all, the homogeneous solution is solved with assumption that the secondary system is overdamped and satisfies with the condition $c^2 > 4m\bar{k}$. This is a reasonable assumption since any equipment hanging on the body of a human will never be critically damped or underdamped. All equipment will attain a zero velocity soon after the human comes to a static position. Therefore, the general solution is given as

$$r_i(t) = \mathrm{C}_{1i}\mathrm{e}^{-(\alpha-\beta_i)t} + \mathrm{C}_{2i}\mathrm{e}^{-(\alpha+\beta_i)t} \tag{3.30}$$

where $\mathrm{C}_{1i}$and C_{2i} are constants

$$\alpha = \frac{c}{2m} \text{ and } \beta_i = \frac{1}{2m}\sqrt{c^2 - 4m\bar{k}_i}$$

Since RHS of Eq. (3.28) is constant the particular solution is easily obtained.

$$r_{pi} = \frac{F_i}{\bar{k}_i} \tag{3.31}$$

Therefore, according to Eq. (3.30) and Eq. (3.31) solution $r(t)$and $\dot{r}(t)$ are

$$r_i(t) = \mathrm{C}_{1i}\mathrm{e}^{-(\alpha-\beta_i)t} + \mathrm{C}_{2i}\mathrm{e}^{-(\alpha+\beta_i)t} + \frac{F_i}{\bar{k}_i} \tag{3.32}$$

$$\dot{r}_i(t) = -(\alpha-\beta_i)\mathrm{C}_{1i}\mathrm{e}^{-(\alpha-\beta_i)t} - (\alpha+\beta)\mathrm{C}_{2i}\mathrm{e}^{-(\alpha+\beta_i)t}$$

If initial conditions when $i = 0$ are assumed that

$$r(0) = r_0 = 0 \tag{3.33}$$

$$\dot{r}(0) = \dot{r}_0 = 0$$

Constants C_{1i} and C_{2i} can be calculated with initial conditions such as:

$$\mathrm{C}_{1i} = \frac{\left(r_i\lambda_{2i} - \dot{r}_i - \frac{F_i\lambda_{2i}}{\bar{k}_i}\right)}{\lambda_{2i} - \lambda_{1i}} \tag{3.34}$$

$$\mathrm{C}_{2i} = \frac{\left(r_i\lambda_{1i} - \dot{r}_i - \frac{F_i\lambda_{1i}}{\bar{k}_i}\right)}{\lambda_{1i} - \lambda_{2i}}$$

where $\lambda_{1i} = -\alpha + \beta_i,\ \lambda_{2i} = -\alpha - \beta_i\ (i = 0,1,\ldots \mathrm{n}-1)$

and *i* is time output.

For initial verification purposes, it is assumed that $\boldsymbol{\theta_1}$ and $\boldsymbol{\theta_2}$ are input from MATLAB/SimMechanics. Eventually, these parameters will come from a predictive dynamics solution.

In order to validate the equations and understand the effect of time step on the accuracy of obtained results, a few numerical tests were performed. Next, the motion of the secondary mass and reaction force between two-link pendulum and spring-mass-damper systems are plotted and compared for 3 seconds with different time step ($t_s = 0.01, 0.001$ and 0.0001). These are shown in Figure 3-7, Figure 3-8 and Figure 3-9. Initial conditions are given $r = \dot{r} = 0$, $\theta_1 = -\frac{\pi}{4}$, $\dot{\theta}_1 = 0$ and $\theta_2 = \dot{\theta}_2 = 0$. By decreasing time step, it is seen that the approximate solution is getting closer to SimMechanics solution. This test also serves as a guide to understand the maximum time step that can be allowed for a desired accuracy in predictive dynamics while solving the two systems simultaneously. While the equations are being integrated using numerical solver, the reaction forces on the primary system due to the presence of secondary system are assumed to be constant during each time step. Hence, the error in the two solutions is larger as the time step increases.

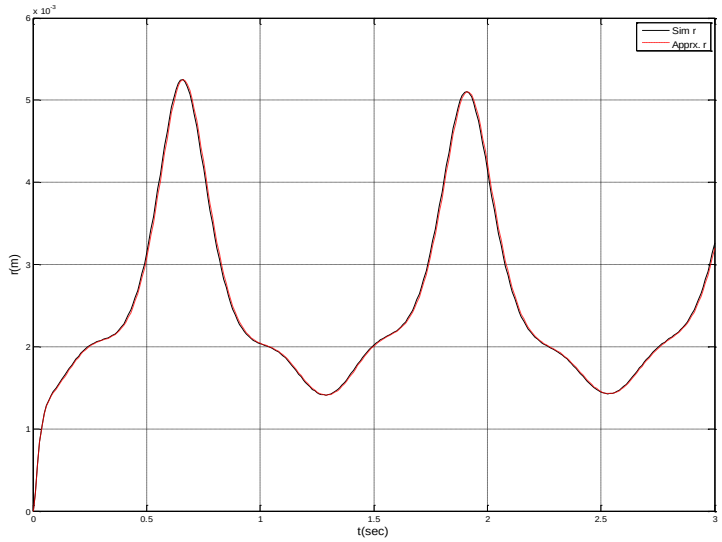

a) Displacement, r, of secondary system

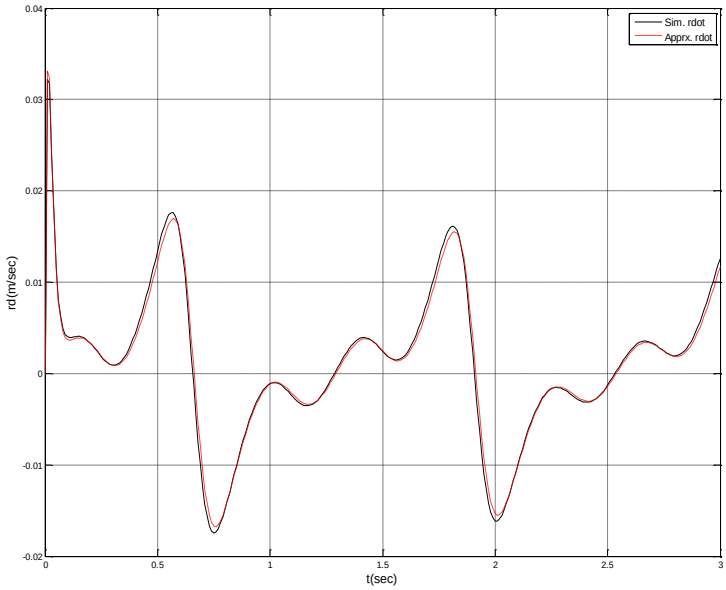

b) Velocity, $\dot{r}$, of secondary system

Figure 3-7 Approximate solution of equations of motion VS SimMechanics solution with time step 0.01 sec

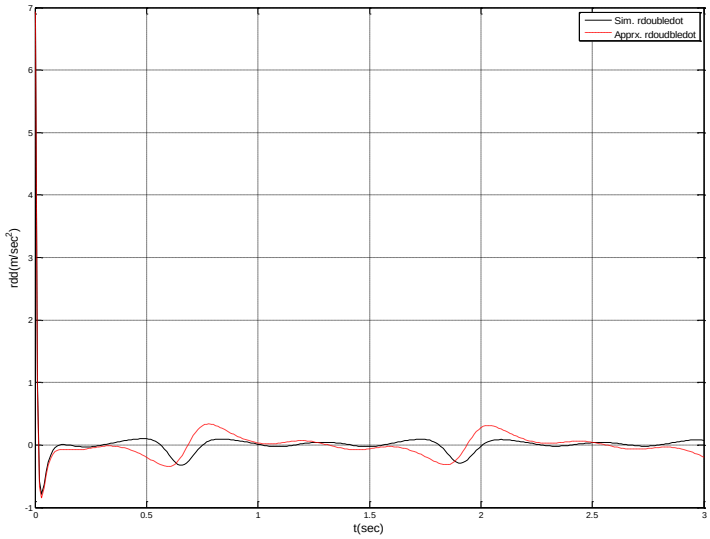

c) Acceleration, $\ddot{r}$, of secondary system

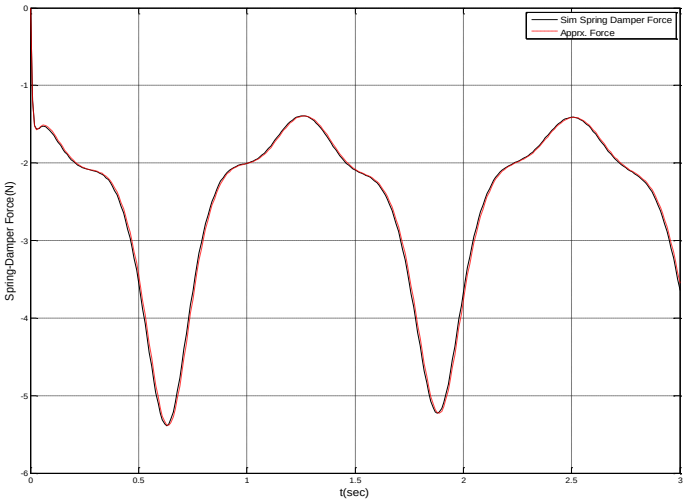

d) Reaction force from secondary system to primary system

Figure 3-7 continued

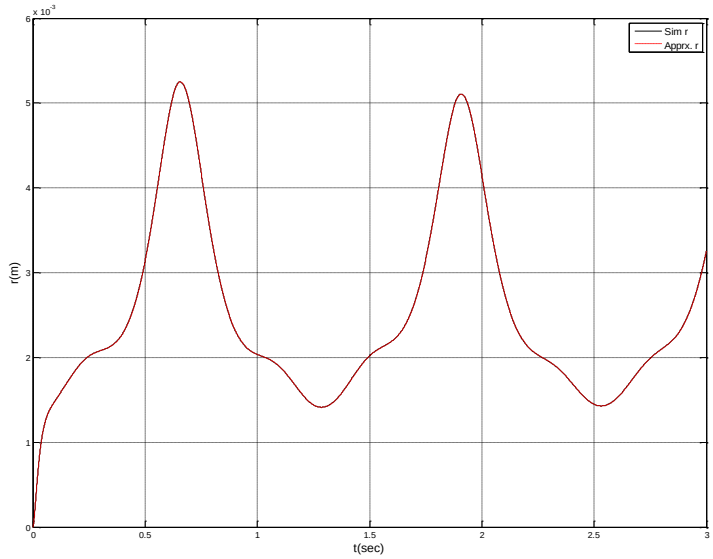

a) Displacement, r, of secondary system

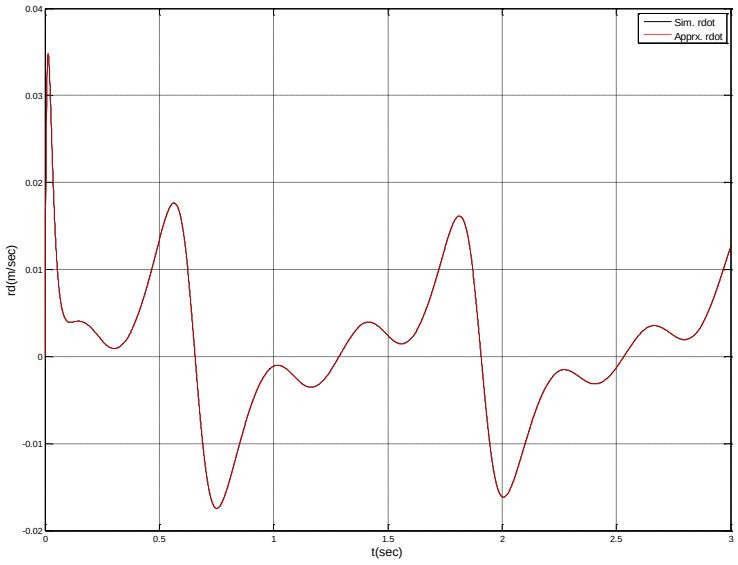

b) Velocity, $\dot{r}$, of secondary system

Figure 3-8 Approximate solution of equations of motion VS SimMechanics solution with time step 0.001 sec

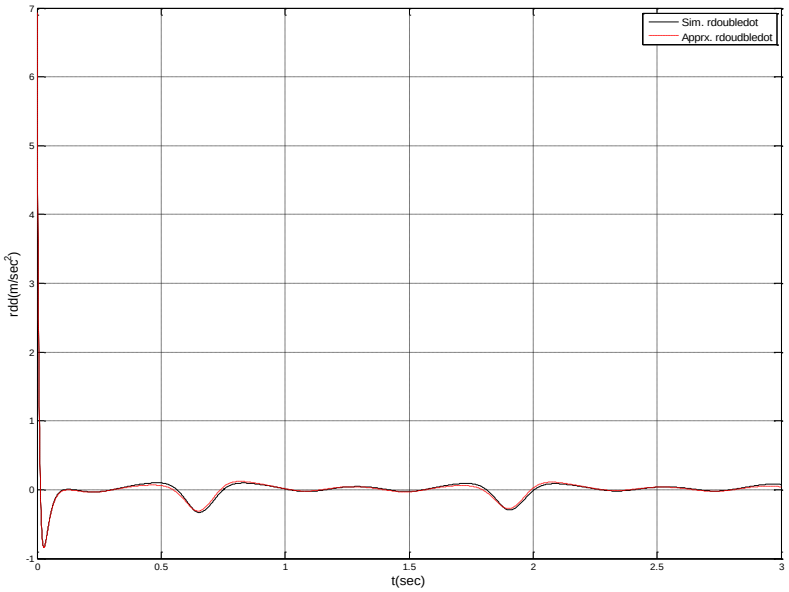

c) Acceleration, $\ddot{r}$, of secondary system

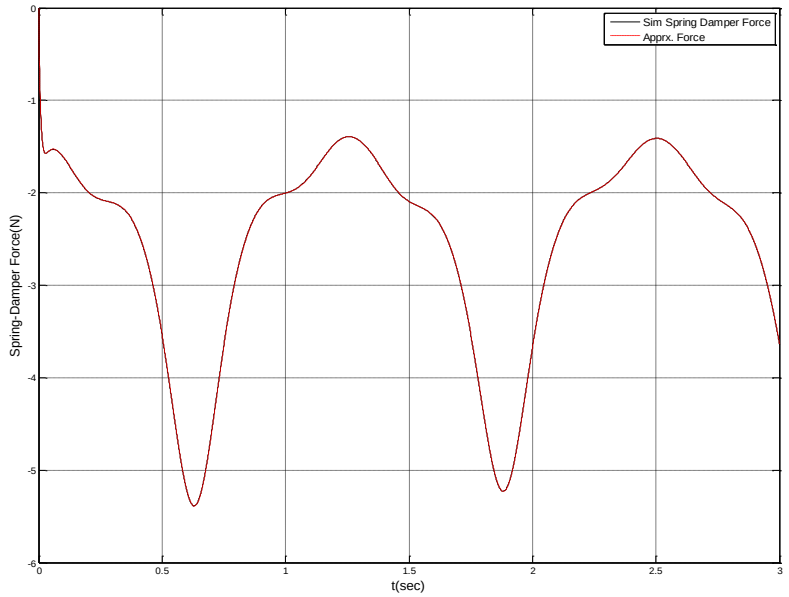

d) Reaction force from secondary system to primary system

Figure 3-8 continued

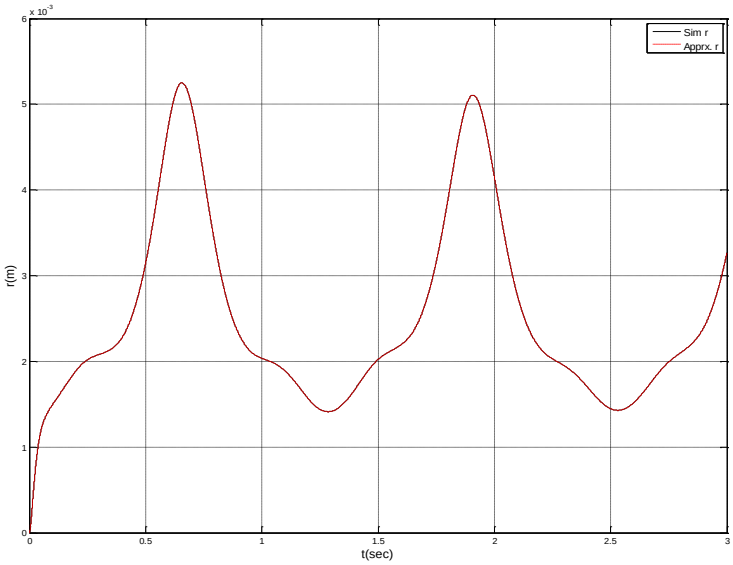

a) Displacement, r, of secondary system

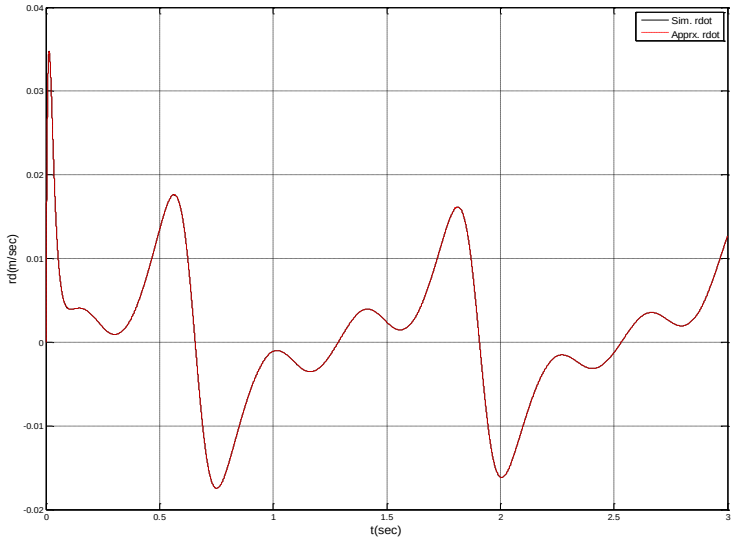

b) Velocity, $\dot{r}$, of secondary system

Figure 3-9 Approximate solution of equations of motion VS SimMechanics solution with time step 0.0001 sec

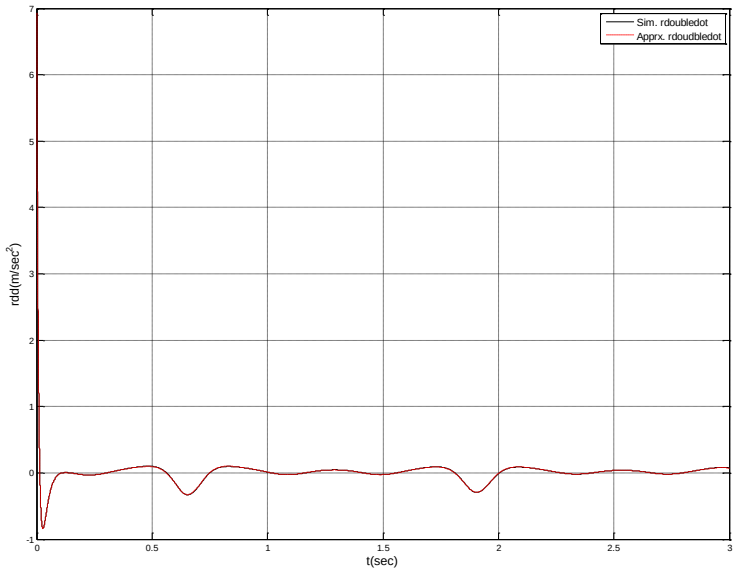

c) Acceleration, $\ddot{r}$, of secondary system

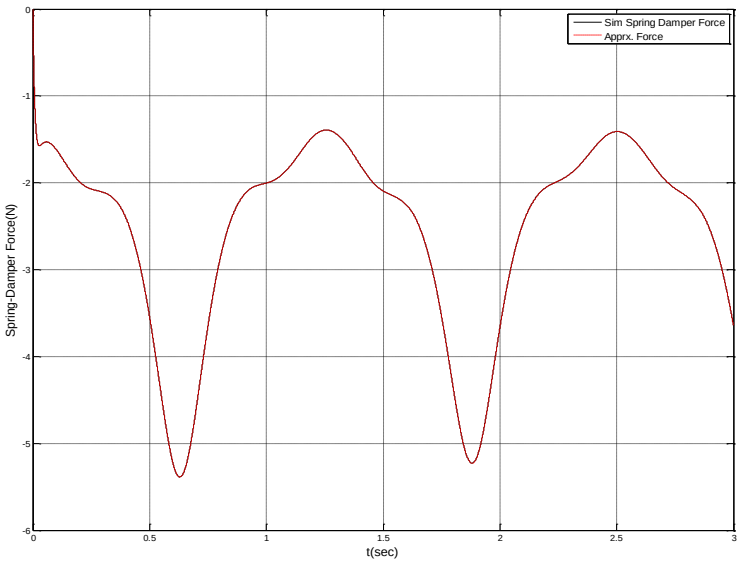

d) Reaction force from secondary system to primary system

Figure 3-9 continued

In the foregoing results, the black line corresponds to the profiles obtained using SimMechanics solution while the red line corresponds to the profiles obtained by using the new approach. In each case (a), (b) and (c) shows the plots of displacement, velocity, and acceleration as a function of time while (d) shows the reaction force at the attachment point as a function of time. As we can see, with larger time step there is more error in the solution due to the approximation of constant reaction forces throughout the time.

3.5 Solution of primary system with known secondary system motion

In this section, it is assumed that the displacement of the secondary system, $\boldsymbol{r}$, is known and the motion of primary system, $\boldsymbol{\theta_1}$ and $\boldsymbol{\theta_2}$, is determined. In this case, the two equations of motion of the two link primary system with external forces, Eq. (3.24) and Eq. (3.25) can be solved simultaneously by using ODE45 (RK4 method) with the same initial condition in Section 3.4. First of all, Eq. (3.24) and Eq. (3.25) can be rewritten as full equation matrix form as:

$$\mathbf{B}\begin{bmatrix}\ddot{\theta}_1\\ \ddot{\theta}_2\end{bmatrix} = \mathbf{d} \tag{3.35}$$

$$\text{where } \mathbf{B} = \begin{bmatrix}b_{11} & b_{12}\\ b_{21} & b_{22}\end{bmatrix} \text{and } \mathbf{d} = \begin{bmatrix}d_1\\ d_2\end{bmatrix}$$

This second order equation can be expressed in the first order form as:

$$\mathbf{A}\dot{\mathbf{p}} = \mathbf{b} \tag{3.36}$$

$$\text{where } \mathbf{A} = \begin{bmatrix}1 & 0 & 0 & 0\\ 0 & b_{11} & 0 & b_{12}\\ 0 & 0 & 1 & 0\\ 0 & b_{21} & 0 & b_{22}\end{bmatrix}$$

$$\mathbf{p} = \begin{bmatrix}p_1\\ p_2\\ p_3\\ p_4\end{bmatrix} = \begin{bmatrix}\theta_1\\ \dot{\theta}_1\\ \theta_2\\ \dot{\theta}_2\end{bmatrix} \text{ so that } \dot{\mathbf{p}} = \begin{bmatrix}\dot{p}_1\\ \dot{p}_2\\ \dot{p}_3\\ \dot{p}_4\end{bmatrix} = \begin{bmatrix}\dot{\theta}_1\\ \ddot{\theta}_1\\ \dot{\theta}_2\\ \ddot{\theta}_2\end{bmatrix} \text{ and } \mathbf{b} = \begin{bmatrix}p_2\\ d_1\\ p_4\\ d_2\end{bmatrix}$$

Therefore, the first order form of the system of equations is obtained by multiplying $\mathbf{A}^{-1}$ to each side such as:

$$\dot{\mathbf{p}} = \mathbf{A}^{-1}\mathbf{b}$$

This first order form can now be solved using ODE45 solver in MATLAB. Since input $\boldsymbol{r}$ is obtained from the MATLAB/SimMechanics benchmark solution, the converted first order form of equations of motions are solved by MATLAB ODE45 with known $\boldsymbol{r}$. The calculated $\boldsymbol{\theta_1}$and $\boldsymbol{\theta_2}$ are also compared with MATLAB solution with different time step. Similarly, the result are plotted and compared for 3 seconds with different time step ($t_s = 0.01, 0.001$ and 0.0001). These are shown in Figure 3-10, Figure 3-11 and Figure 3-12.

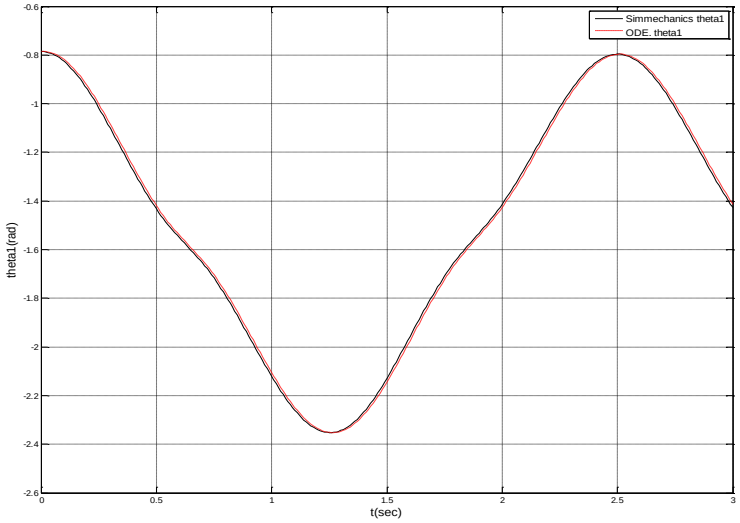

a) Joint angle profile of Link 1, θ_1, plotted against time

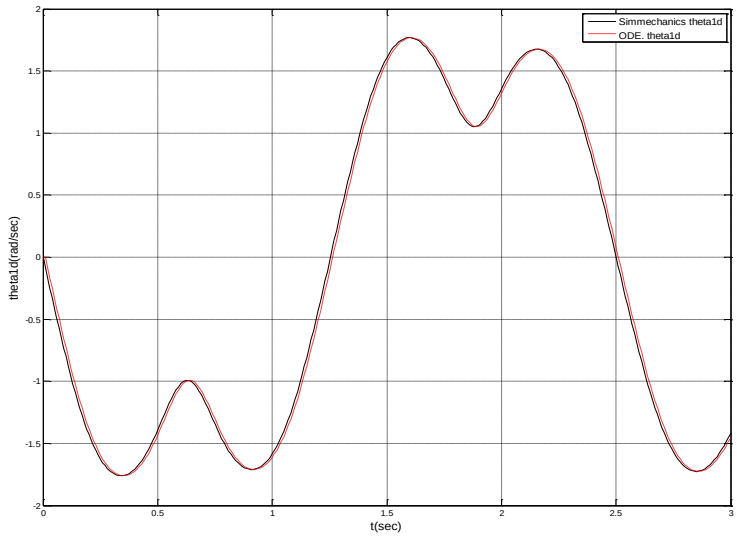

b) Joint velocity profile of Link 1, $\dot{\theta}_1$, plotted against time

Figure 3-10 ODE solution of equation of motion VS SimMechanics solution with time Step 0.01 sec

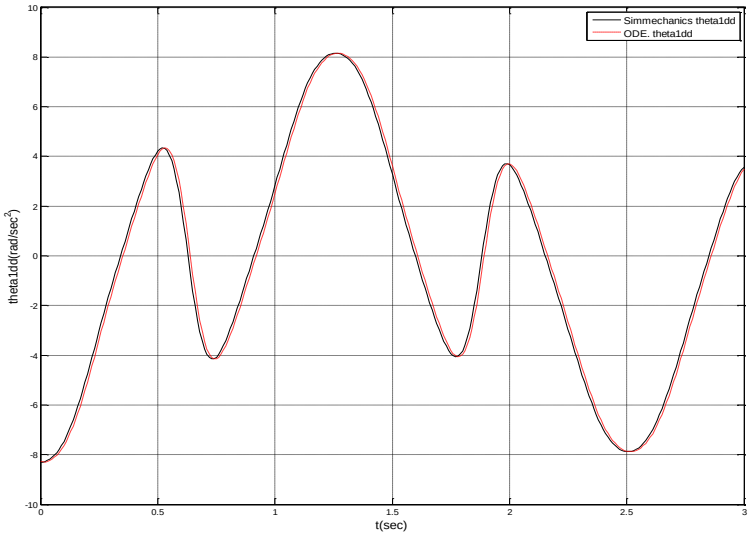

c) Joint acceleration profile of Link 1, $\ddot{\theta}_1$, plotted against time

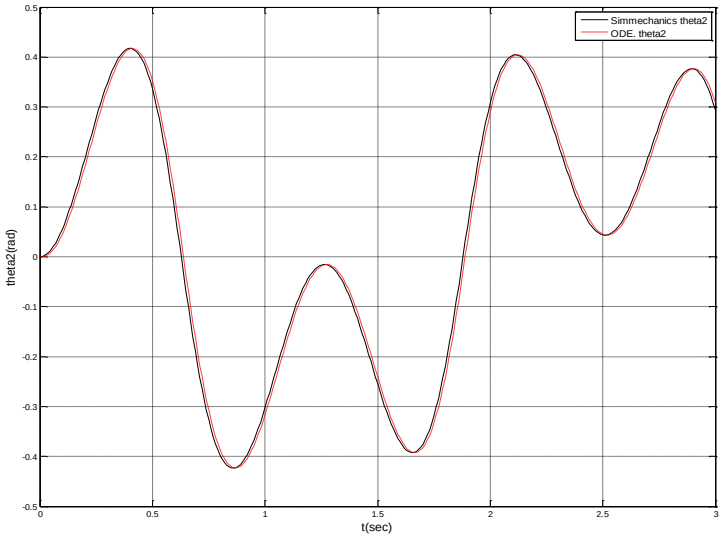

d) Joint angle profile of Link 1, θ_2, plotted against time

Figure 3-10 continued

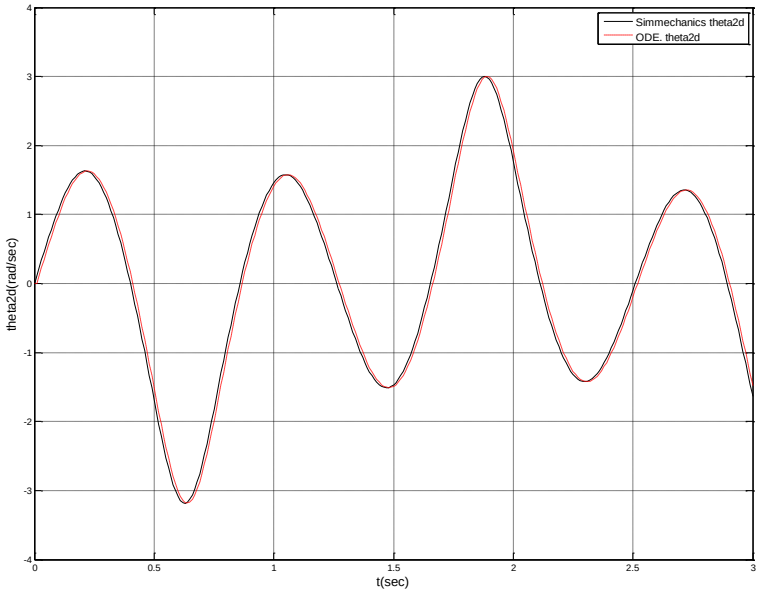

e) Joint velocity profile of Link 1, $\dot{\theta}_2$, plotted against time

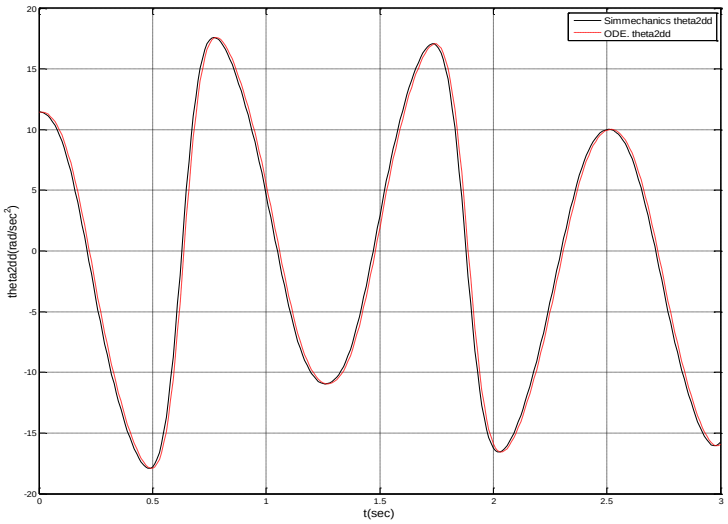

f) Joint acceleration profile of Link 1, $\ddot{\theta}_2$, plotted against time

Figure 3-10 continued

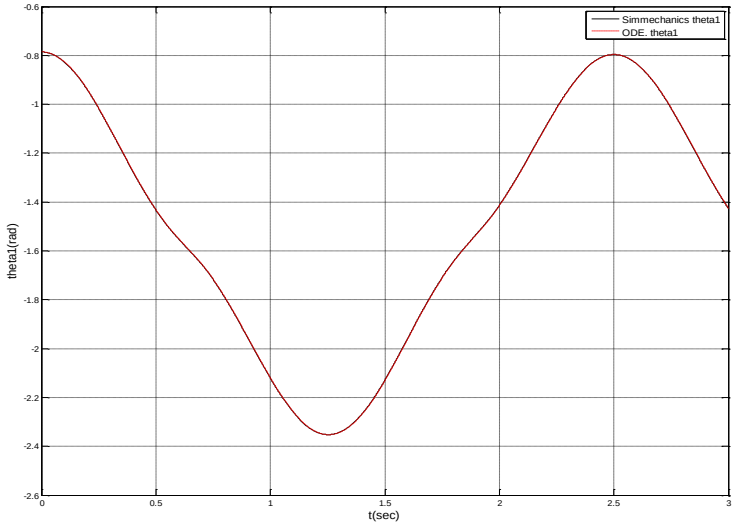

a) Joint angle profile of Link 1, θ_1, plotted against time

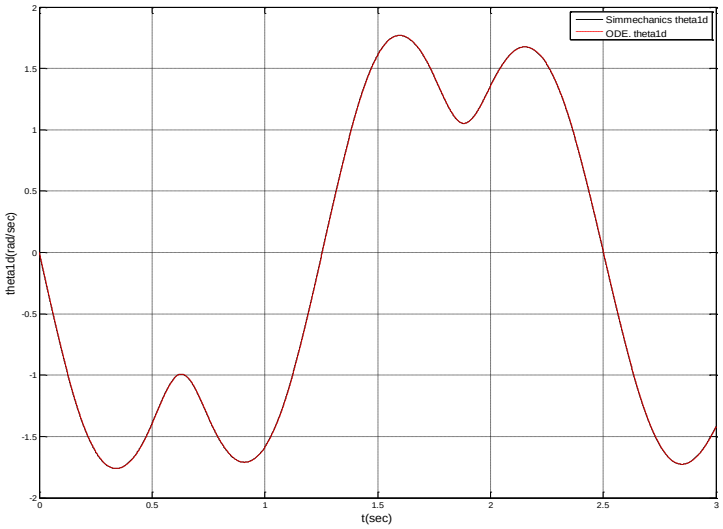

b) Joint velocity profile of Link 1, $\dot{\theta}_1$, plotted against time

Figure 3-11 ODE solution of equation of motion VS SimMechanics solution with time step 0.001 sec

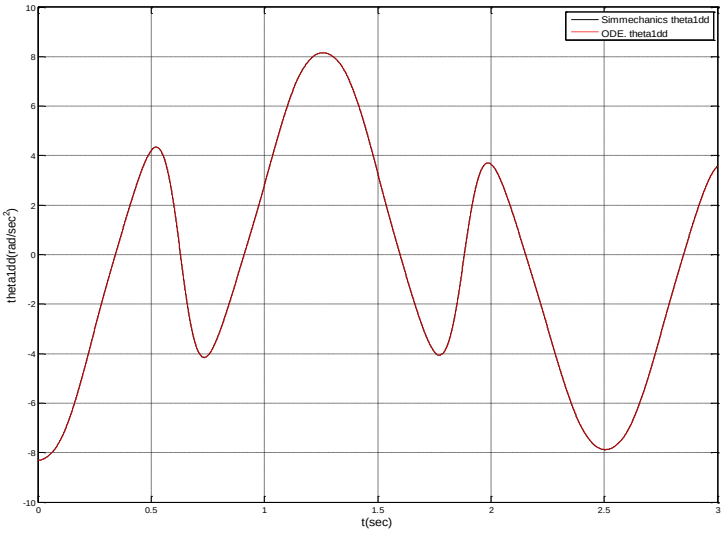

c) Joint acceleration profile of Link 1, $\ddot{\theta}_1$, plotted against time

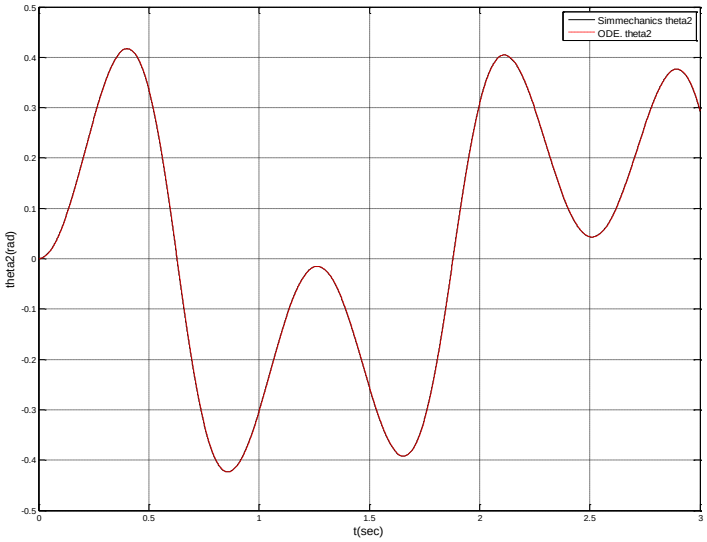

d) Joint angle profile of Link 1, θ_2, plotted against time

Figure 3-11 continued

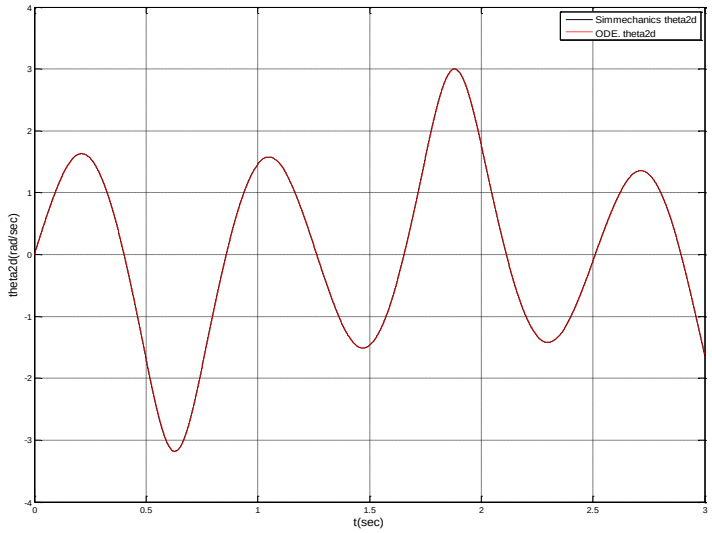

e) Joint velocity profile of Link 1, $\dot{\theta}_2$, plotted against time

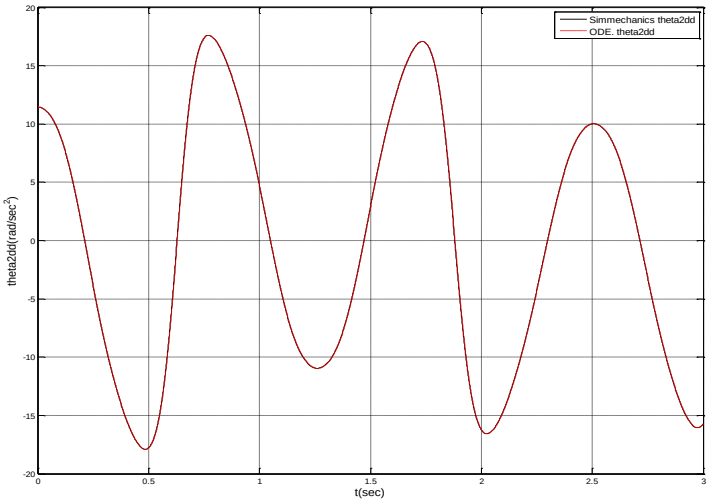

f) Joint acceleration profile of Link 1, $\ddot{\theta}_2$, plotted against time

Figure 3-11 continued

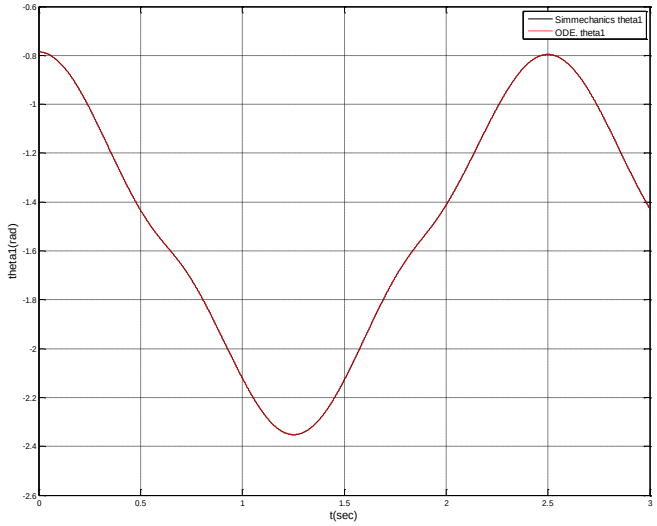

a) Joint angle profile of Link 1, θ_1, plotted against time

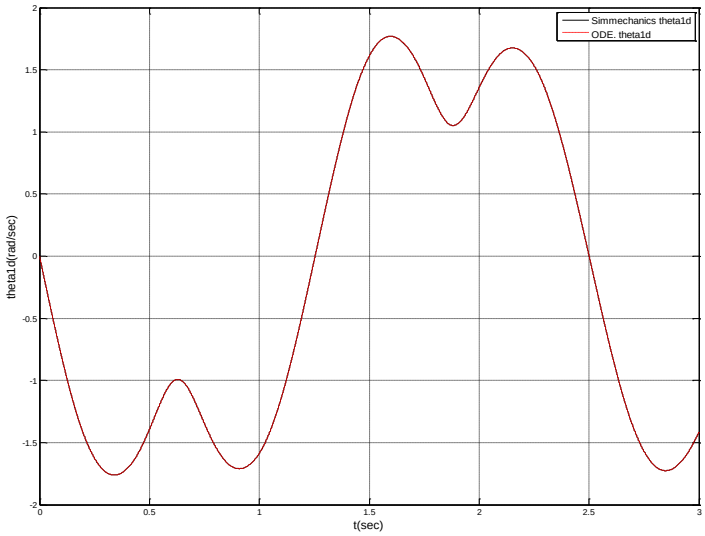

b) Joint velocity profile of Link 1, $\dot{\theta}_1$, plotted against time

Figure 3-12 ODE solution of equation of motion VS SimMechanics solution with time step 0.0001 sec

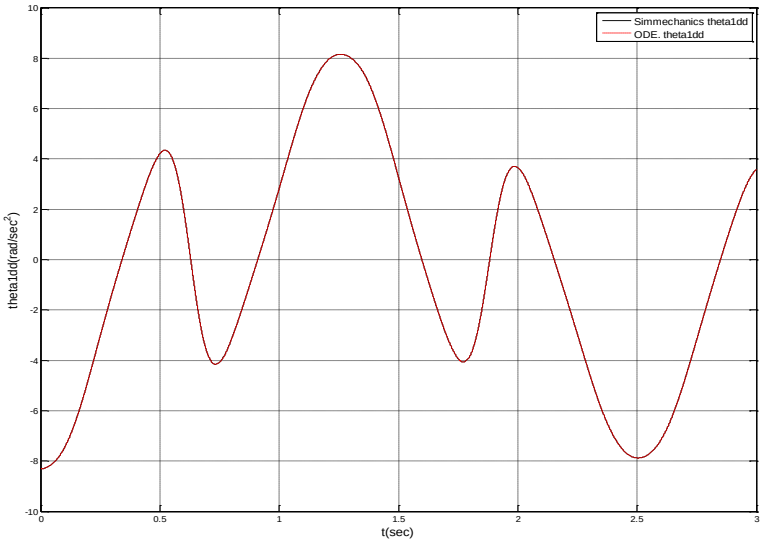

c) Joint acceleration profile of Link 1, $\ddot{\theta}_1$, plotted against time

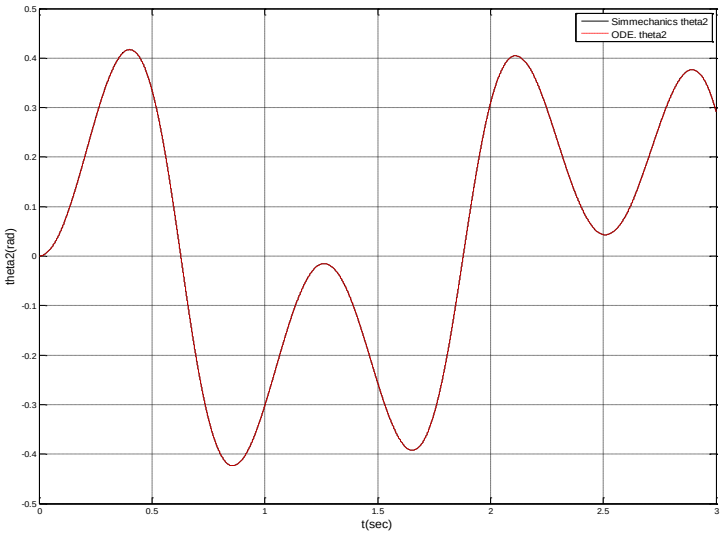

d) Joint angle profile of Link 1, θ_2, plotted against time

Figure 3-12 continued

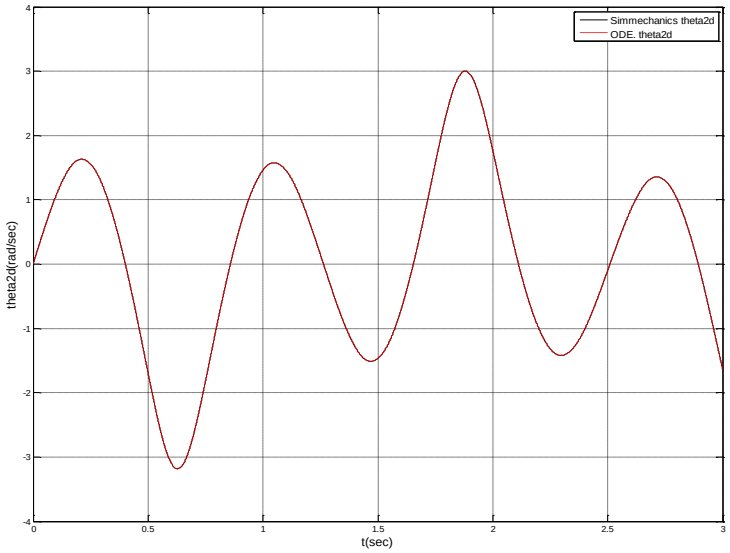

e) Joint velocity profile of Link 1, $\dot{\theta}_2$, plotted against time

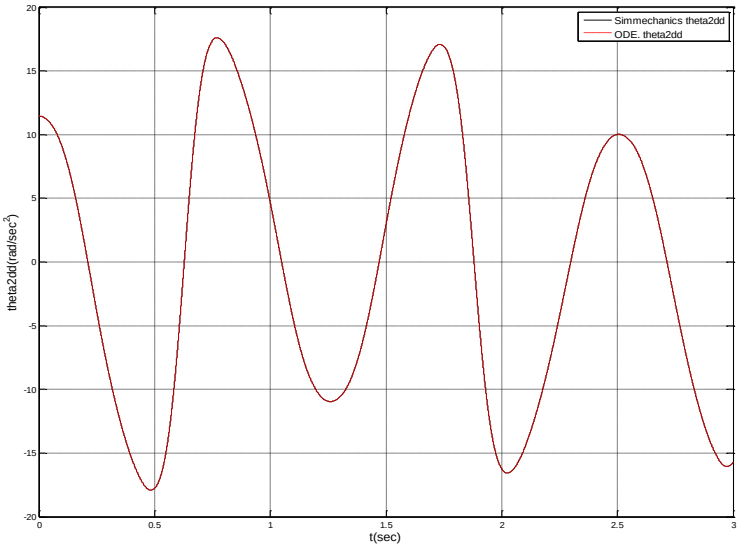

f) Joint acceleration profile of Link 1, $\ddot{\theta}_2$, plotted against time

Figure 3-12 continued

Each figure above corresponds to solution for a different time step. As we can see from the results that the different time steps do not affect the motion of the primary system much. These results show that for a rough estimate, the primary system can be considered as driving and the secondary system can be considered as driven system. In this case, the error in the two solutions is decreased by reducing time step of integration.

CHAPTER 4

PREDICTIVE DYNAMICS APPLICATION OF REACTION FORCE AND MOMENT

In this chapter, the predictive dynamics approach of solving the equations of motion of large systems such as human models is introduced. This algorithm must be adapted so that the backpack modeled as the spring-mass-damper (SMD) system obtains the motion from human model and the reaction forces and moments from the SMD system can be applied to the human. Predictive dynamics is a DAE solving algorithm applied to digital human modeling and simulation. It is an optimization-based methodology to predict physically-realistic human motions while avoiding integrating the typical differential algebraic equations. Instead, the methodology imposes the equations of motions as constraints in the optimization problem, thus allowing use of highly redundant and anatomically correct joint-based full-body human models with relatively less computational expense. In addition, inequality constraints on the generalized coordinates are easily treated in this approach. Each human motion task is characterized by an objective function and a unique set of constraints that define the task. The equations of motion are assembled in a canonical form rather than derived in terms of the total momentum of the system to gain numerical efficiency and stability (Lankarani *et al*, 2001). Various task motions have been predicted and validated using the predictive dynamics approach with physics-based digital human model (Abdel-Malek *et al*, 2008)

4.1 Predictive dynamics

In predictive dynamics approach, the general equations of motion for the representative mathematical model of the primary system are written as:

$$\mathrm{f}(q, \dot{q}, \ddot{q}, t) = \mathbf{F} \qquad (4.1)$$

where $q, \dot{q}, \ddot{q} \in \mathbf{R}^N$ are the state variables, and $\mathbf{F} \in \mathbf{R}^N$ are the generalized forces. This dynamics problem is defined over the time domain $\Omega = (T_0, T)$ with boundary, $\Gamma = \{T_0, T\}$,$t \in \Omega$, t being the time and the symbol $\dot{(\cdot)}$ indicating derivative with respect to t. The superscript N represents the number of DOF of the skeletal model. This primary system could be a 3D human model or a planar two link simple pendulum.

Forward dynamics calculates the motion (q, $\dot{q}$ and $\ddot{q}$) from the force **F** by integrating Eq. (4.1) with the specified initial conditions. In contrast, inverse dynamics computes the associated force **F** that leads to a prescribed motion for the system. The two procedures are depicted in Figure.1 (a) and (b). For simplicity, we use only q to represent kinematics of the system.

In practice, it is difficult to measure complete displacement q and force **F** histories accurately for a biomechanical system with many DOF, especially involving a complex motion. This is because the experimental measurement is either not accurate enough or too expensive to achieve the required accuracy. However, the boundary conditions and some state response of the system might be available. In this case, neither forward dynamics nor inverse dynamics can be applied to the bio-system **S** directly. As a consequence, the predictive dynamics procedure is proposed to solve these types of problems. The basic idea is to formulate a nonlinear optimization problem based on the physics of the motion (the dynamics of the motion). An appropriate performance measure (objective function) for the biomechanical system is defined and minimized subject to the available information about the system that imposes various constraints. In this case, both displacement and force histories are unknown and need to be identified by solving the optimization problem. This is called the predictive dynamics approach and is formulated for the system as follows.

$$\min_{q,\boldsymbol{F}} \quad J(q, \mathbf{F}, t)$$

$$\textit{s.t.:} \quad \mathbf{F}\text{-}\,\mathrm{f}(q, t) = 0$$

$$\mathbf{g}(\Upsilon) \leq 0$$

$$q^L \leq q \leq q^U$$

$$\mathbf{F}^L \leq \mathbf{F} \leq \mathbf{F}^U$$

where **g** are the constraints defined based on the available information Υ about the biomechanical system. q and **F** are subject to their lower and upper bounds, respectively. For the biomechanical system, the objective function is usually called the performance measure.

4.2 Solution algorithm

The predictive dynamics algorithm used to solve primary system must be modified to account for the calculated reaction forces and moments from the secondary system as explained through flowchart of Fig 4-1. The flow chart includes basic predictive dynamics steps including optimization process. The two blocks highlighted in yellow must be introduced to the predictive dynamics algorithm so that it can be used to simulate the motion of human as well as the equipment. The outputs, reaction forces and moment, are dependent upon kinematic information and secondary system properties such as spring constant, damping coefficient, secondary system mass and initial length. The first block outside the optimization loop reads the information about the secondary system. If there are more than one secondary systems, this block would read information about all secondary systems. The second highlighted yellow block in the optimization loop calculates and applies the reaction forces and moment at each iteration for each time step. Hence, the secondary system is solved multiple times iteratively until the solution converges.

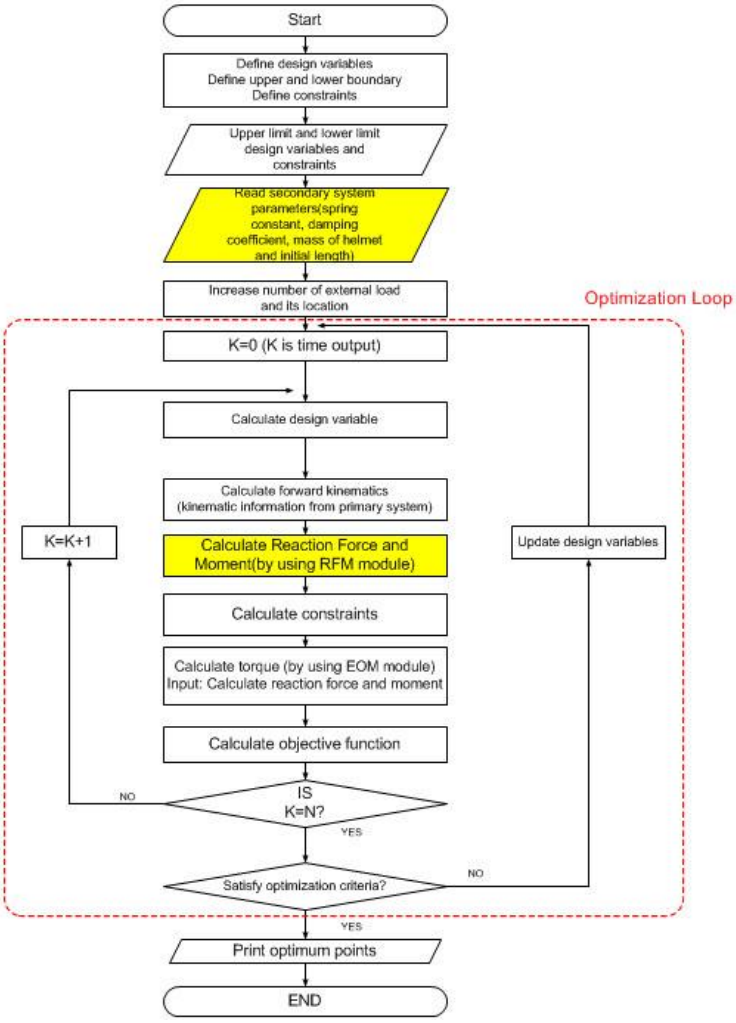

Figure 4-1 Predictive dynamics flow chart with caculation of reaction and moment

4.3 Interaction beween two systems

Figure 4-2 shows an example of how primary and secondary systems interact by applying updated reaction forces and moment. In this case, primary system is expressed as two-link pendulum. Since kinematic information of the primary system is provided at each time k in the predictive dynamics algorithm, the reaction forces and moment are also updated at time k. That is, reaction forces and moment at time k are calculated with given kinematic information at time k and the calculated reaction forces and moment affect the primary system. The kinematic information is updated at time k+1 and it will

generate updated reaction forced and moment at time k+1. Therefore, this calculation loop will keep going until end of time.

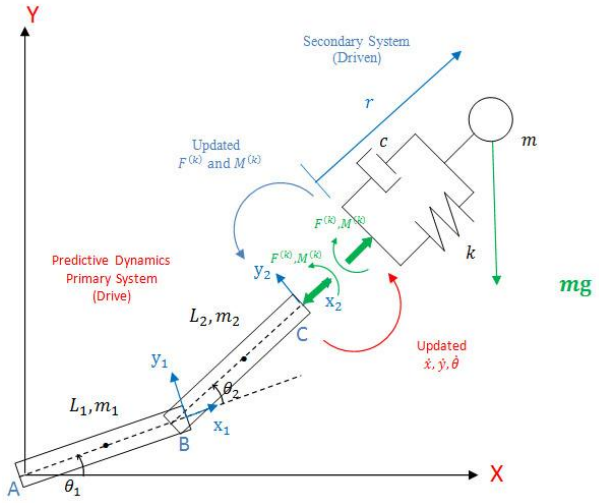

Figure 4-2 Application of reaction forces and moment to primary system and update kinematic information of primary system

4.4 Calculation of secondary system motion

As shown in Figure 4-2, the reaction forces and moment from the secondary system to the primary system are calculated at each time. The horizontal progression in the figure Figure 4-3 shows how the values for each iteration are calculated as the time progresses. The equation of motion of secondary system and reaction forces and moment calculation are already observed in Section 3.4.

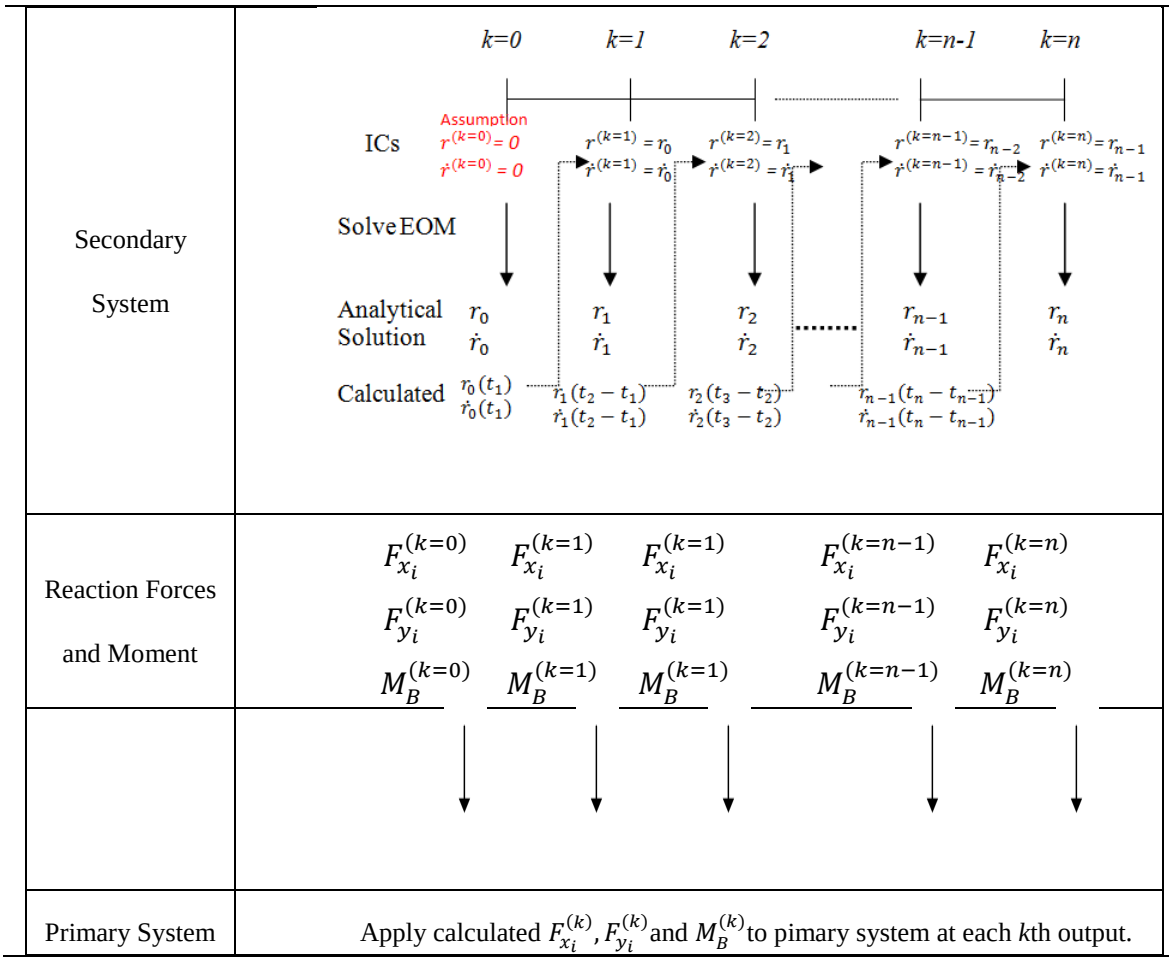

Figure 4-3 Application of reaction forces and moment

In Section 3.4, the assumptions were already introduced to solve secondary system. The first assumption is secondary system satisfies over-damped condition which is $c^2 > 4m\bar{k}$. In addition, initial conditions for the secondary system are zero. Finally, primary system states are constant.

At time output $k = 0$, equation of motion of primary system is solved with assumed initial condition for the secondary system. Then, the equation of motion for the secondary system is solved using the kinematic information from the primary system. The reaction forces and moments at time k+1 are then calculated based on the properties of the secondary system and the displacement obtained by solving the equations of

motion. Calculated reaction forces and moment are applied to primary system and calculated analytical solution is updated to initial conditions for next time output $k = 1$. This procedure keeps doing at the end of time.

CHAPTER 5

NUMERICAL RESULT OF SIMULATING TWO LINK SIMPLE PENDULUM WITH SPRING-MASS-DAMPER SYSTEM AS EQUIPMENT

The new approach to simulate the motion of the primary and secondary systems while solving the equations of motion independently using predictive dynamics was discussed in Chapter 4. This approach is implemented on the two link simple pendulum system with equipment attached using a spring mass damper system. The results of the secondary system displacement and the reaction forces due to this secondary system on the primary system are then compared against the benchmark solution.

During optimization phase of predictive dynamics method, the primary system solution is obtained in the first iteration by assuming zero force due to the presence of secondary system. Then, using the kinematic information about the system, the secondary system is solved and the reaction forces are updated for each time-step. Then, the primary system is again solved for new motion for current iteration while applying the updated reaction forces due to the secondary system. This iterative process is repeated until the system converges.

5.1 Vertical initial position

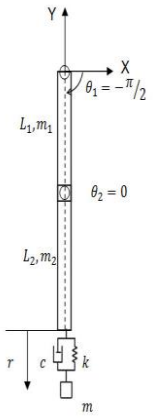

Figure 5-1 Vertical initial position

The full system was solved for three different initial conditions and for two different time steps. The Figure 5-1 shows vertical initial position of the system. This was a simple test case with a known solution. Since the primary system is vertical and the secondary system is hanging off the primary system, the primary system should stabilize and come to rest. The optimization problem formulated for this case is as follows:

Find joint angle profiles

$$min. \quad \sum \int \tau_i \, dt$$

$$s.t \quad -\pi \leq \theta_i \leq \pi$$

$$\theta_1(0) = -\pi/2, \theta_2(0) = 0$$

$$\dot{\theta}_1(0) = \dot{\theta}_2(0) = 0$$

$$\theta_1(0.9) = -\pi/2, \theta_2(0.9) = 0$$

$$\dot{\theta}_1(0.9) = \dot{\theta}_2(0.9) = 0$$

The result of this simulation is shown in Figure 5-2.

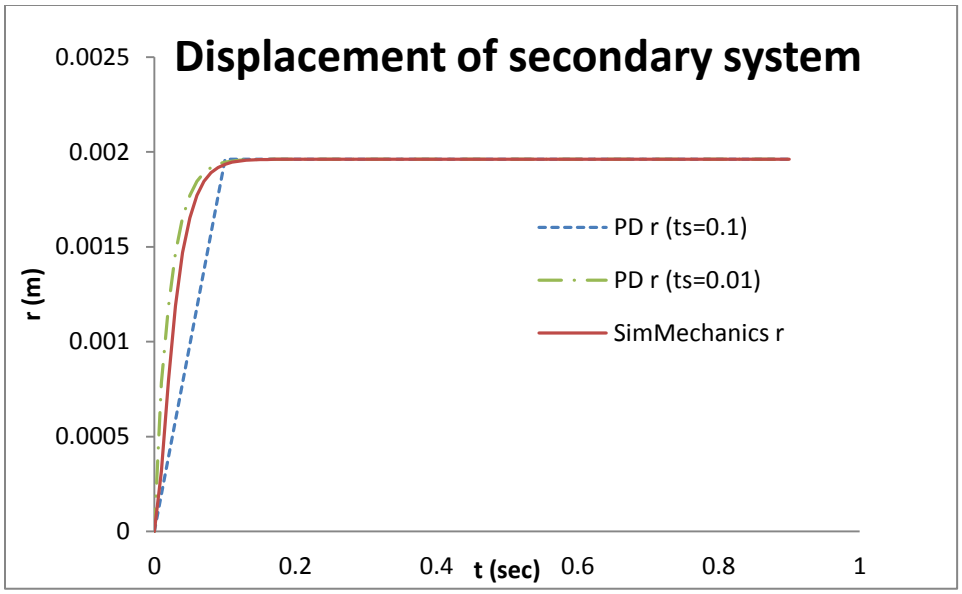

a) Comparison of displacement of secondary system

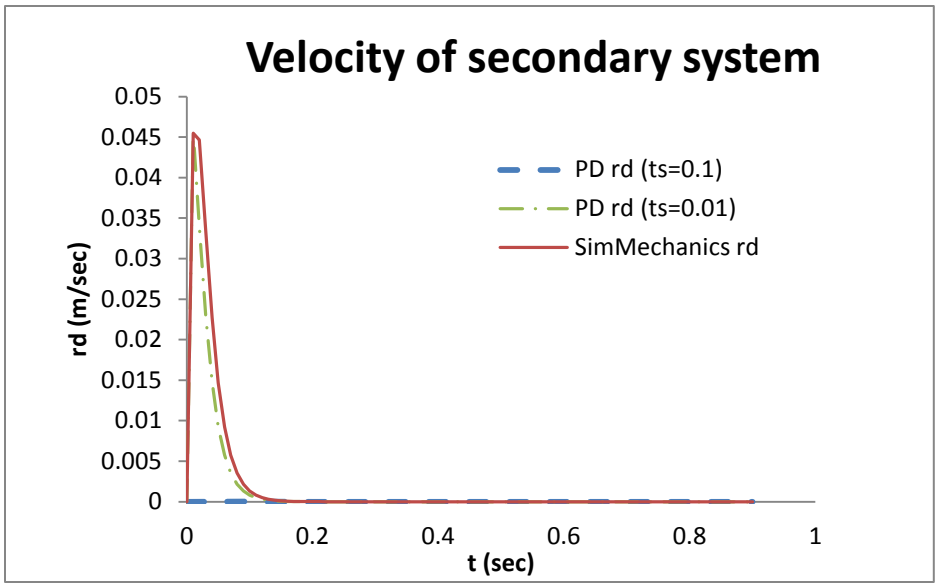

b) Comparison of velocity of secondary system

Figure 5-2 Comparison of calculated solution and benchmark solution (vertical initial position)

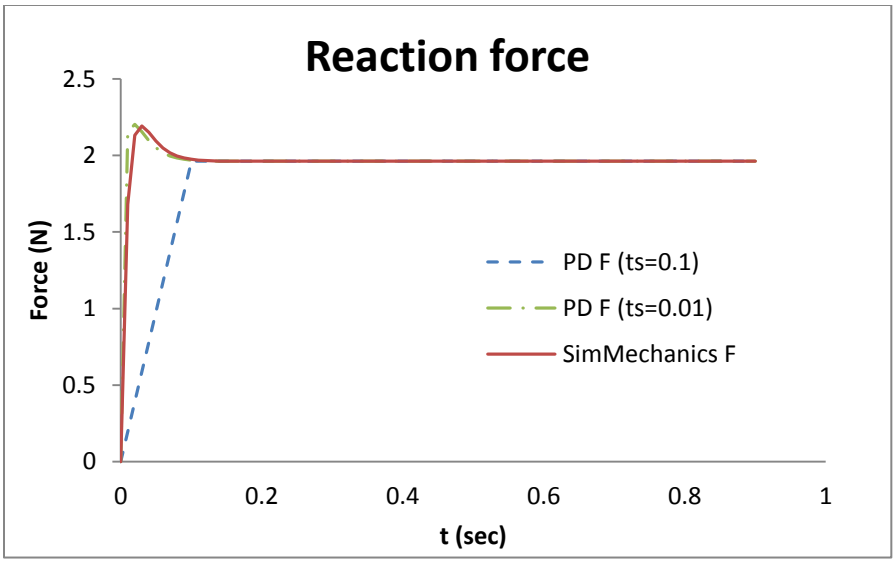

c) Comparison of reaction force on primary system due to the presence of secondary system

Figure 5-2 continued

5.2 Intermediate initial position

In this case study, it was assumed that the first link makes a 45 degrees angle, $\theta_1 = -\pi/4, \theta_2 = 0$, with the horizontal at time t = 0. The configuration of the system is shown in Figure 5-3.

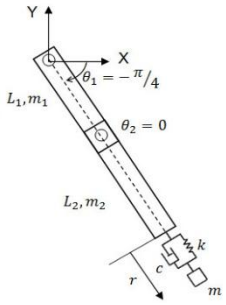

Figure 5-3 Random$\left(\theta_1 = -\pi/4, \theta_2 = 0\right)$ initial position

Similarly, the optimization problem for this case can be formulated as:

Find joint angle profiles

$$min. \quad \sum \int \tau_i \, dt$$

$$s.t \quad -\pi \leq \theta_i \leq \pi$$

$$\theta_1(0) = \theta_2(0) = 0$$

$$\dot{\theta}_1(0) = \dot{\theta}_2(0) = 0$$

$$\theta_1(0.3) = -0.4894, \theta_2(0.3) = 0\,.5866$$

$$\theta_1(0.5) = -1.0866, \theta_2(0.5) = 0\,.6749$$

$$\theta_1(0.9) = -2.1539, \theta_2(0.9) = -0.31382$$

$$\dot{\theta}_1(0.9) = -4.60498, \;\; \dot{\theta}_2(0.9) = 4.979044$$

The simulation results are shown in Figure 5-4. The primary system has larger motion compared to the case 1. The error in the motion of the secondary system is thus larger than the first case. As can be observed from the graph, the results from new approach matches closely the benchmark SimMechanics solution for about 0.5 seconds and after that, the error increases. Since predictive dynamics tasks only solving the system for single time step, which is mostly around 0.5 seconds long, the application of current approach is promising for such scenarios.

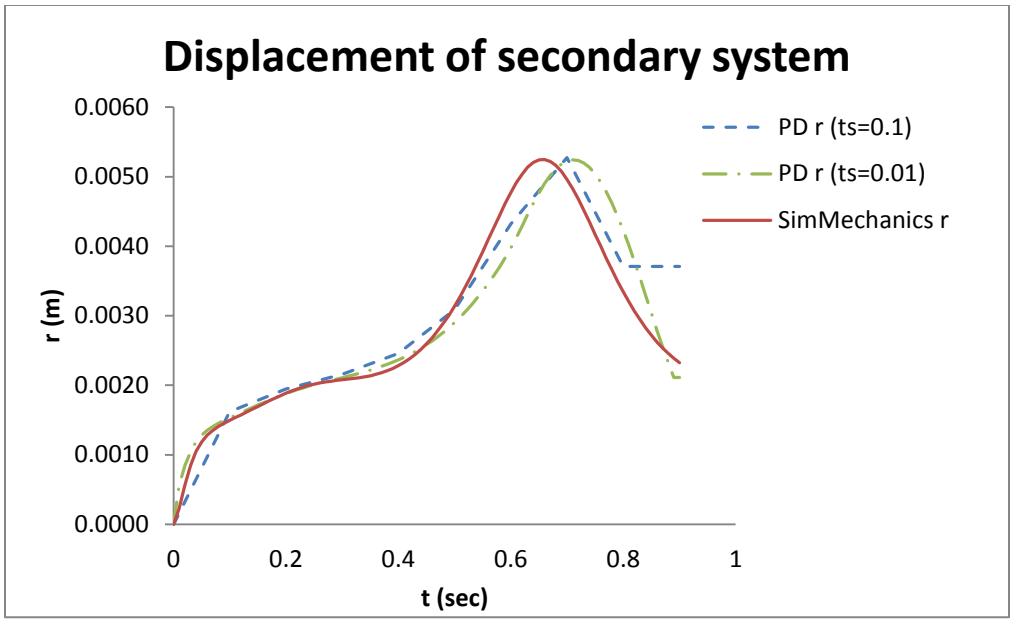

a) Comparison of displacement of secondary system

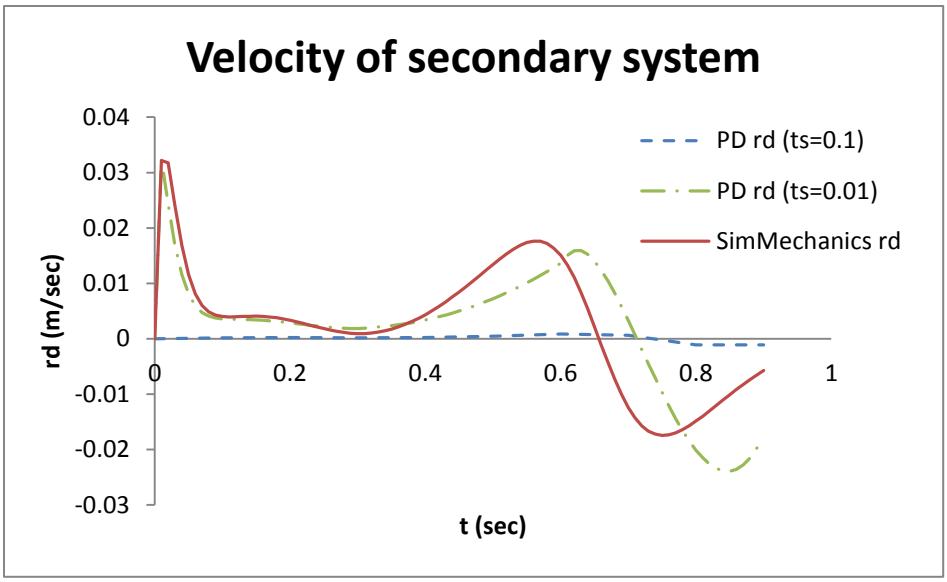

b) Comparison of velocity of secondary system

Figure 5-4 Comparison of calculated solution and benchmark solution (random position) $(\theta_1 = -\pi/4, \theta_2 = 0)$

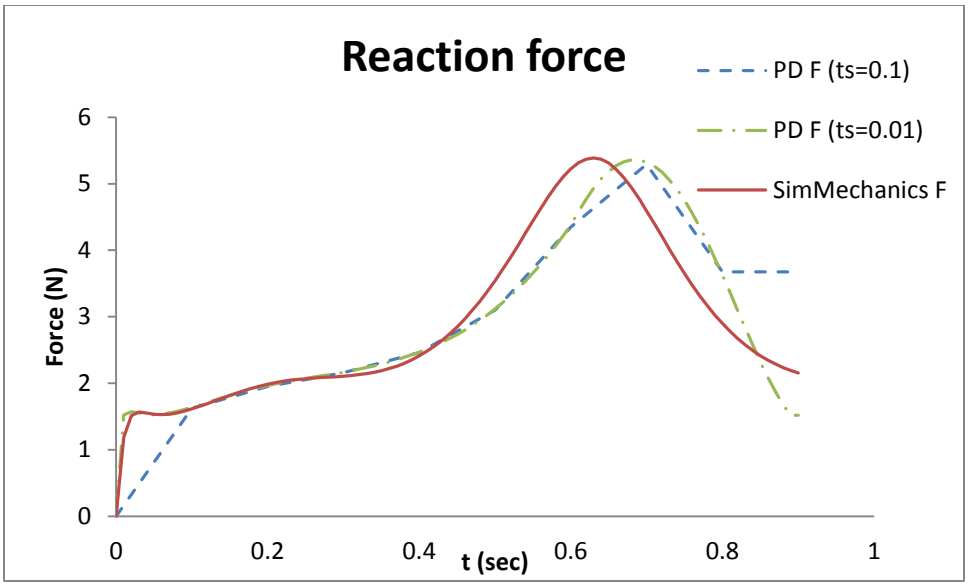

c) Comparison of reaction force on primary system due to the presence of secondary system

Figure 5-4 continued

5.3 Horizontal initial position

The primary system is assumed to be at a horizontal position as shown in Figure 5-5. When dropped under the effect of gravity under this position, the primary system has even larger motion. The system runs three different time step: 0.1 sec, 0.01 sec and 0.0001sec.

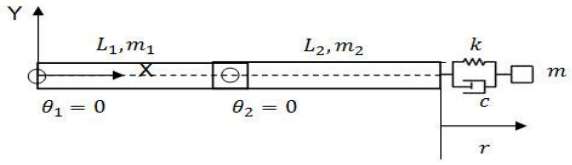

Figure 5-5 Horizontal initial position

The optimization problem for this case can thus, be formulated as:

Find joint profiles

$$min. \quad \sum \int \tau_i \, dt$$

$$s.t \quad -\pi \leq \theta_i \leq \pi$$

$$\theta_1(0) = \theta_2(0) = 0$$

$$\dot{\theta}_1(0) = \dot{\theta}_2(0) = 0$$

$$\theta_1(0.3) = -0.4894, \theta_2(0.3) = 0.5866$$

$$\theta_1(0.5) = -1.0866, \theta_2(0.5) = 0.6749$$

$$\theta_1(0.9) = -2.1539, \theta_2(0.9) = -0.31382$$

$$\dot{\theta}_1(0.9) = -4.60498, \dot{\theta}_2(0.9) = 4.979044$$

5.3.1 History of secondary system motion

The results of this case are shown in Figure 5-6. Because this case is highly nonlinear motion than motion of previous two cases, the error between the solution using the new approach and the benchmark solution is even larger than the previous case. However, the displacement, velocity as well as reaction force follow the same profile. Moreover, the solution matches for the initial 0.5 seconds before it starts diverging.

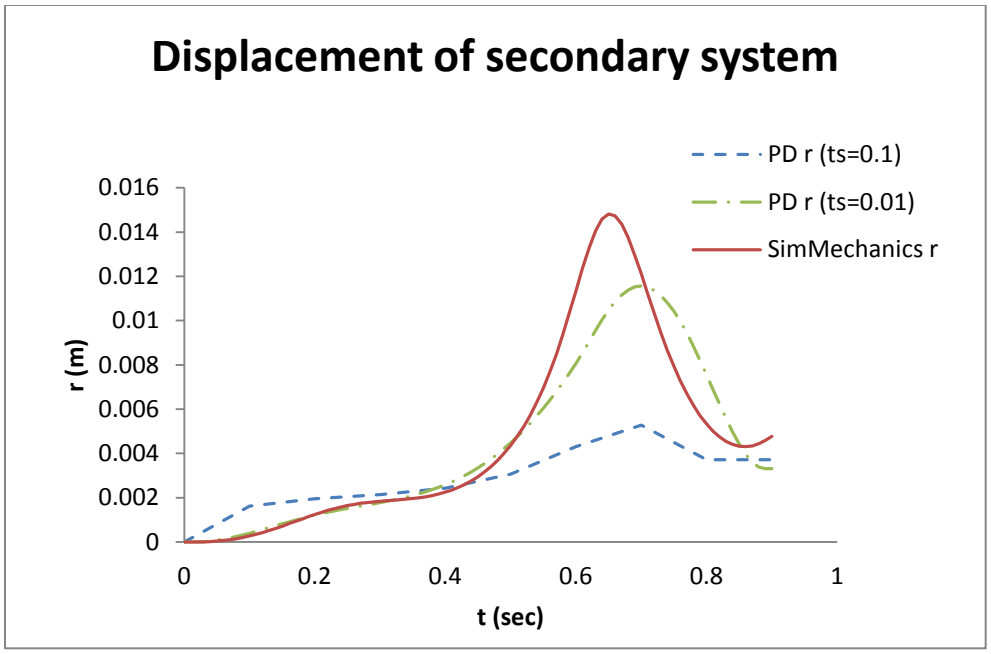

a) Comparison of displacement of secondary system

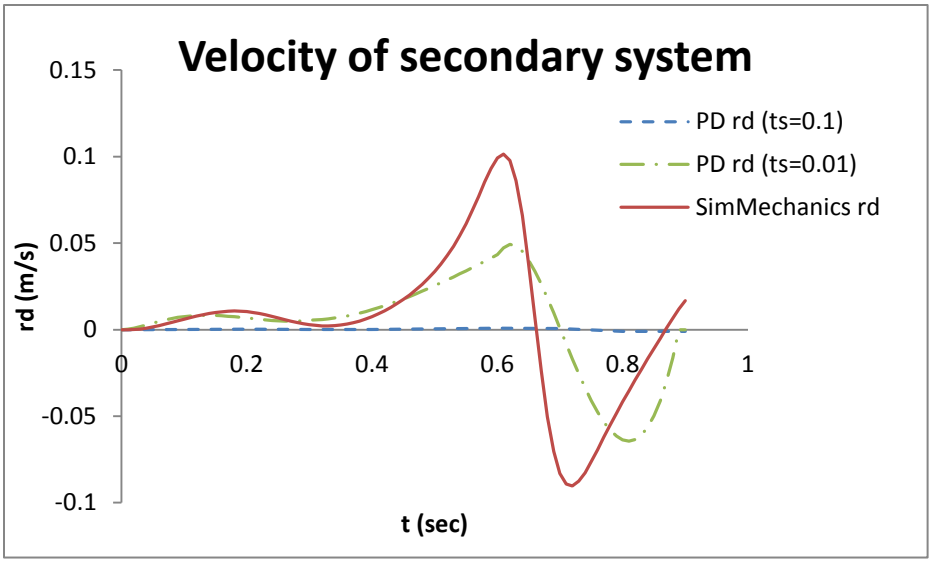

b) Comparison of velocity of secondary system

Figure 5-6 Comparison of calculated solution and benchmark solution (horizontal initial position)

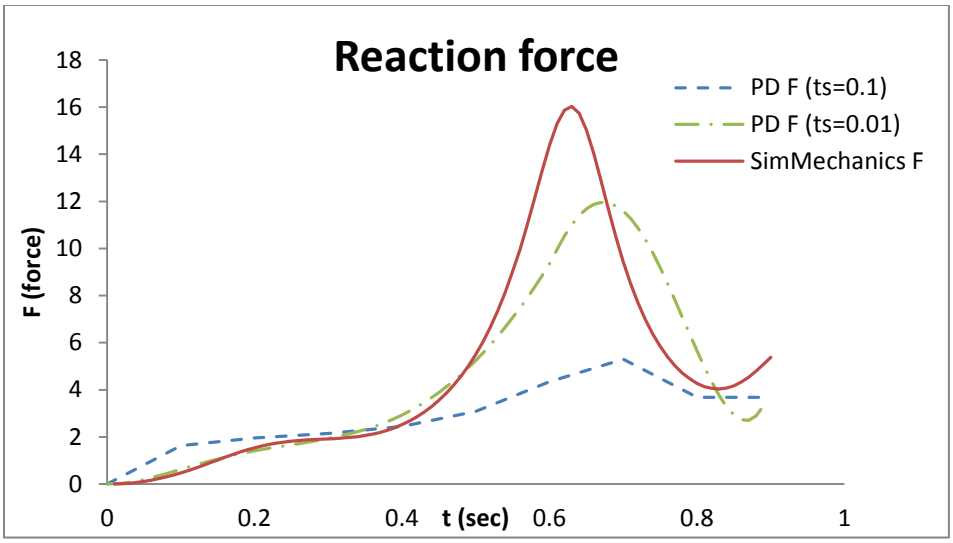

c) Comparison of reaction force on primary system due to the presence of secondary system

Figure 5-6 continued

It seems that the error is dependent on the initial position of the full system. In three different cases, the vertical initial position case shows very good result. Since the primary system is in stationary status, the secondary system motion is only affected by gravity force. On the other hands, the horizontal initial position doesn't show good trend because the motion of primary system is affected too much nonlinear. In case of random initial position case, it shows good trend but there is still error between two solutions. Especially, the error starts to accumulate from 0.4 sec. This error may come from the solution process of equation of motion of the secondary system.

Overall, the secondary system motion is well matched with SimMechanics solution in the order of vertical initial position, random initial position and horizontal initial position. In addition, the displacement of secondary system result shows better trend than velocity of secondary system result. It is obvious that the reaction force shows also good trend because the reaction force is mainly dominated by the spring force.

5.3.2 History of primary system motion

According to the results, it shows that the solution has not been improved much even though time step is decreased from 0.01 sec to 0.0001sec. In other words, the approximation due to the assumption that the states of primary system are constant during the time-step is not the only cause for the error. Hence, the primary system motion profiles were compared against the benchmark solution.

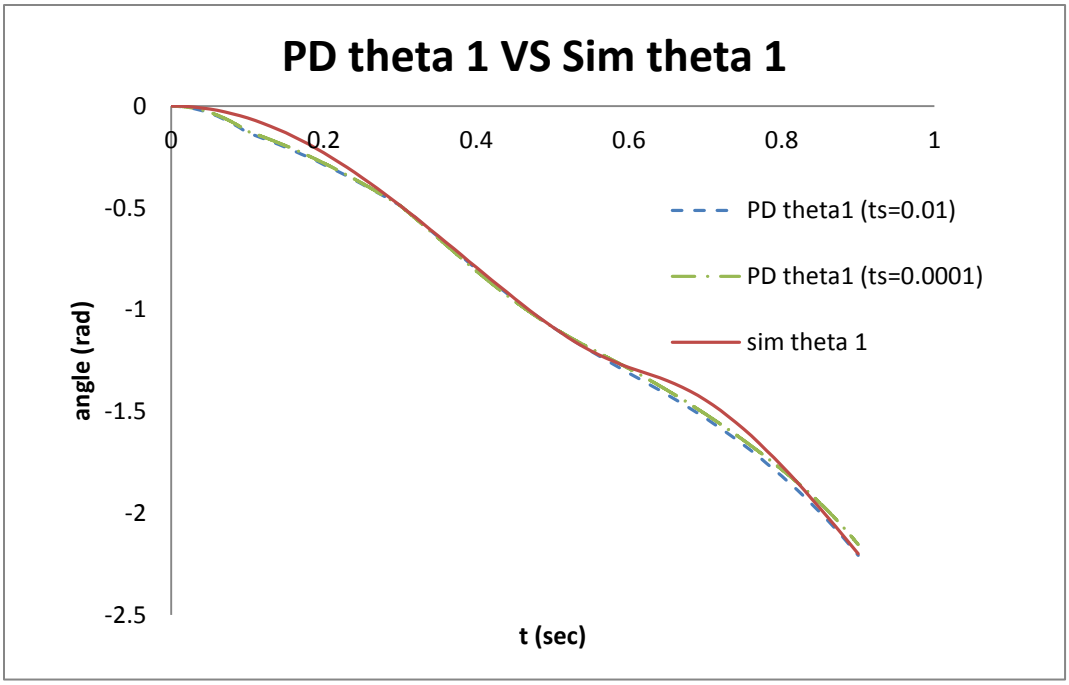

a) Comparison of the first joint angular displacement (θ_1)

Figure 5-7 Comparison of calculated joint angular displacement and benchmark solution

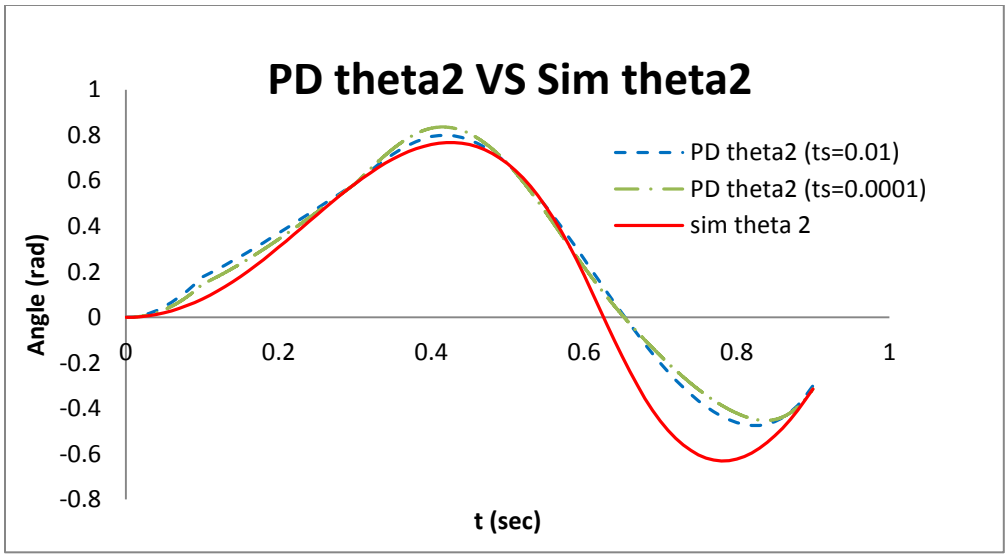

b) Comparison of the second joint angular displacement (θ_2)

Figure 5-7 continued

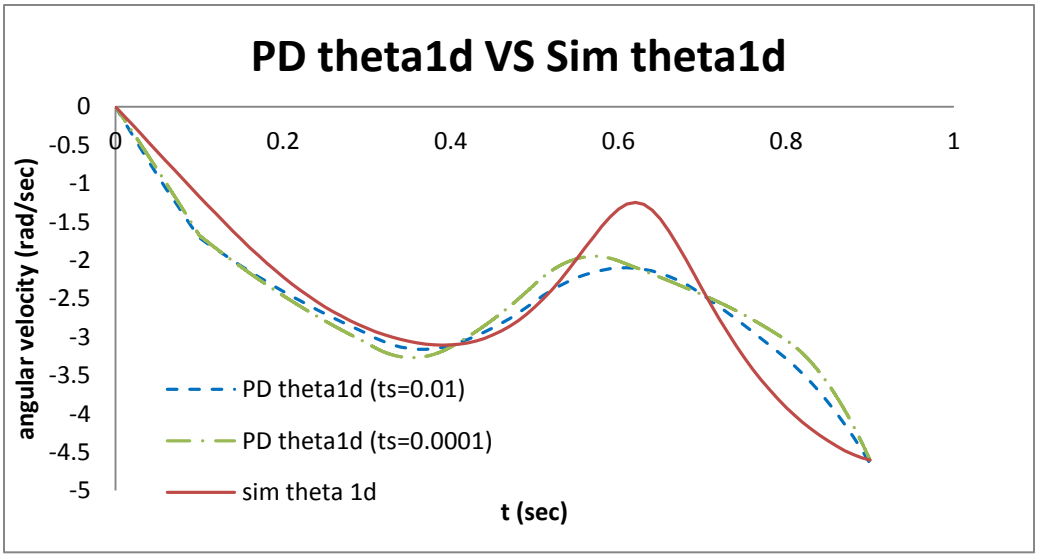

a) Comparison of the first joint angular velocity $(\dot{\theta}_1)$

Figure 5-8 Comparison of calculated joint angular velocity and benchmark solution

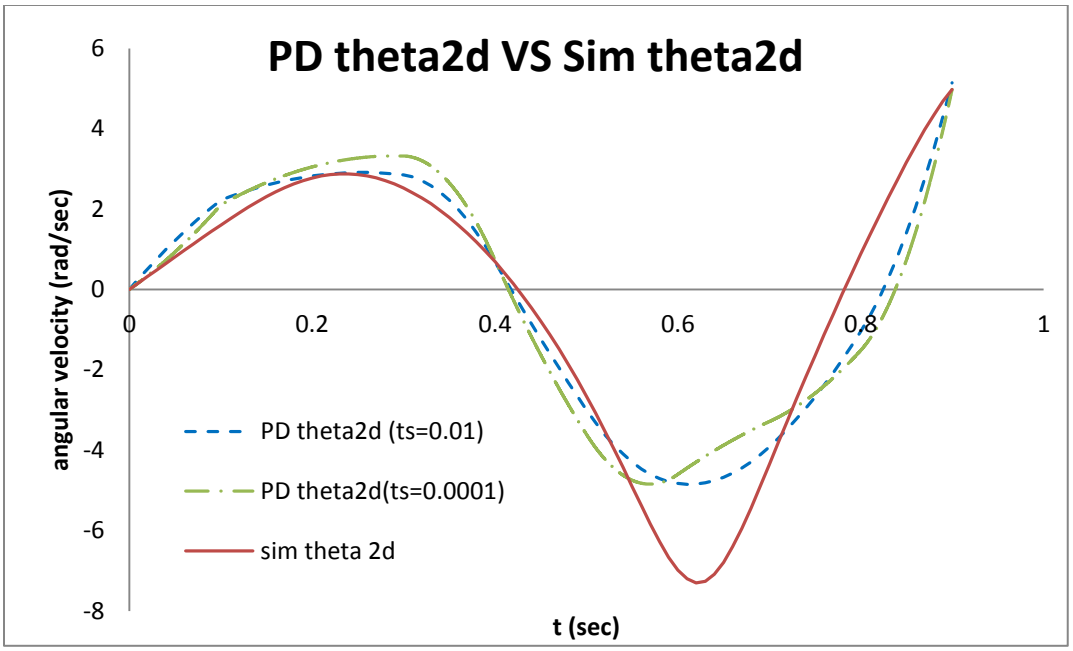

b) Comparison of the second joint angular velocity $(\dot{\theta}_2)$

Figure 5-8 continued

Based on Figure 5-7 and Figure 5-8, the angular displacements show similar trend with benchmark solution. However, the angular velocities have error after 0.4 sec. Therefore, the error of secondary system on Figure 5-8 might be explained by error of angular velocities on Figure 5-8. In detail, the introduced equation of motion for secondary system in Section 3.4 is function of $\boldsymbol{\theta_1}$and $\boldsymbol{\theta_2}$, the secondary system motion error is affected by the primary system motion error, especially angular velocities, in this case.

5.3.3 Follow mocap cost function

Previously, it is proved that the secondary system result is not accurate because the primary system has error from certain time. In other words, the primary system error should be reduced to obtain better result of secondary system motion. In this section, the

new cost function is introduced to solve primary system so that the primary system motion shows less error than solution with previous cost function. The new cost function is called Follow mocap cost function which is shown below:

min. $\sum(\theta_{d_i} - \theta_i)^2$

where θ_{d_i} are the desired joint angle from the benchmark SimMechanics solution.

5.3.4 History of primary system motion with new cost function

The given problem, objective function and constraints are shown as follows.

Find joint profiles

min. $\sum(\theta_{d_i} - \theta_i)^2$

where θ_{d_i} are from SimMechanics

s.t $-\pi \leq \theta_i \leq \pi$

$\theta_1(0) = \theta_2(0) = 0$

$\dot{\theta}_1(0) = \dot{\theta}_2(0) = 0$

$\theta_1(0.3) = -0.4894, \theta_2(0.3) = 0.5866$

$\theta_1(0.5) = -1.0866, \theta_2(0.5) = 0.6749$

$\theta_1(0.9) = -2.1539, \theta_2(0.9) = -0.31382$

$\dot{\theta}_1(0.9) = -4.60498, \dot{\theta}_2(0.9) = 4.979044$

The motion of primary system is shown below.

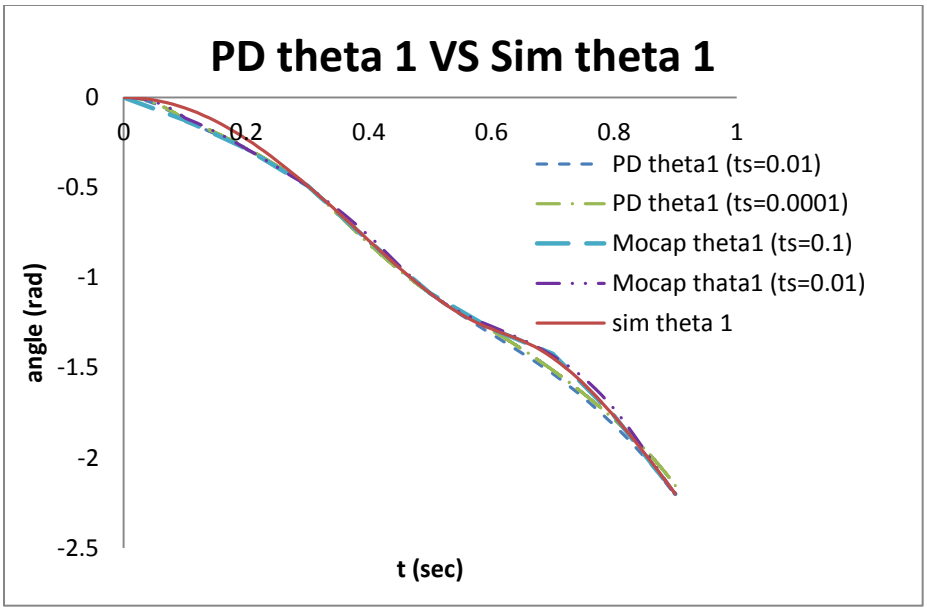

a) Comparison of the first joint angular displacement (θ_1)

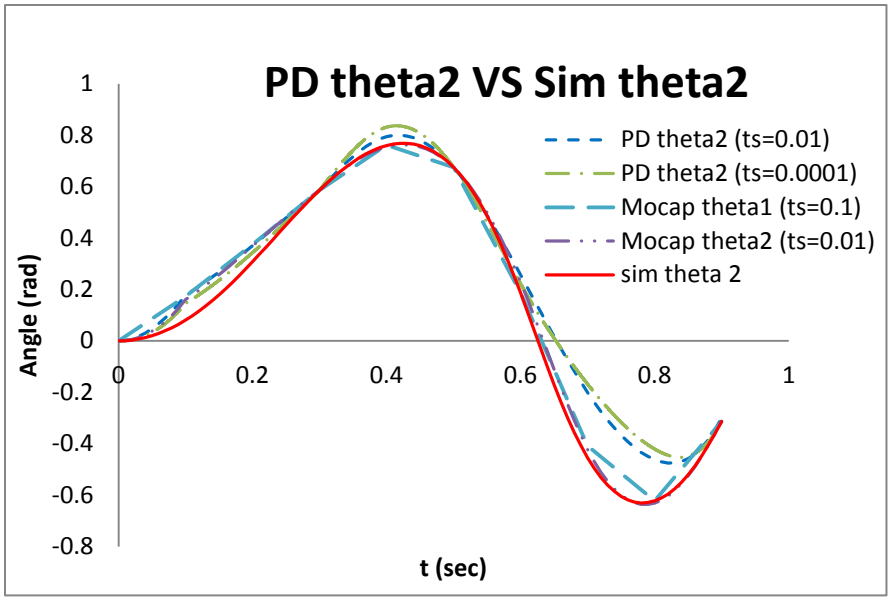

b) Comparison of the second joint angular displacement (θ_2)

Figure 5-9 Comparison of calculated joint angular displacement and benchmark solution with new cost function

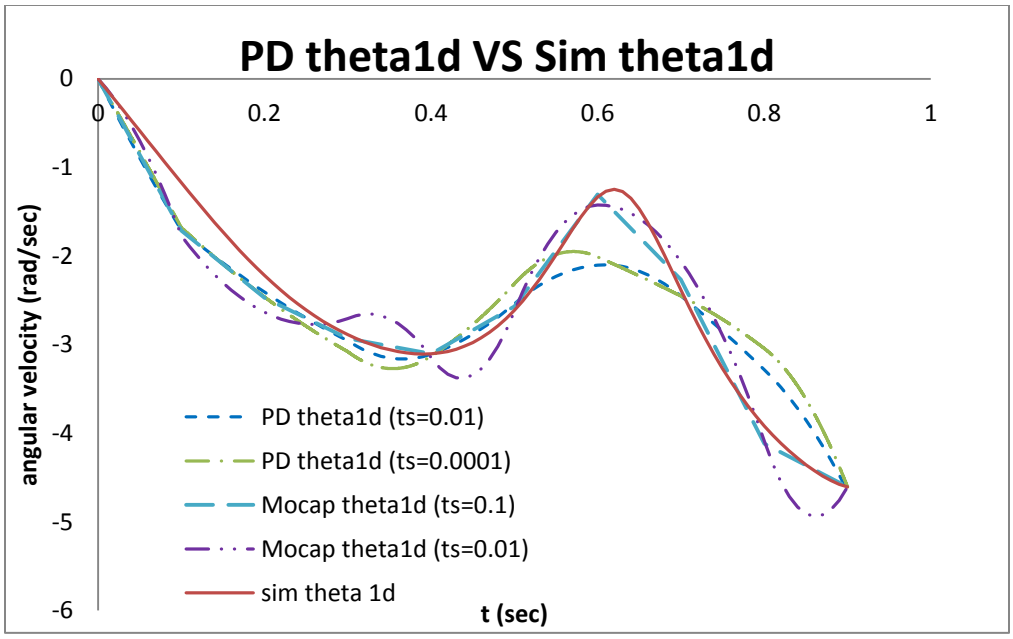

a) Comparison of the first joint angular velocity $(\dot{\theta}_1)$

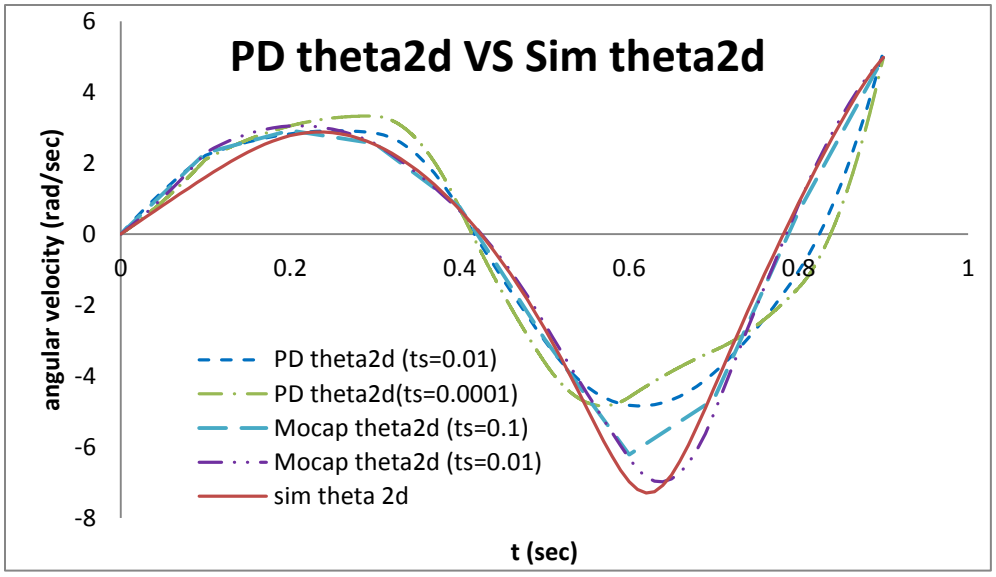

b) Comparison of the second joint angular velocity $(\dot{\theta}_2)$

Figure 5-10 Comparison of calculated joint angular velocity and benchmark solution with new cost function

According to Figure 5-9 and Figure 5-10, it is shown that the primary system solution with follow mocap function shows better result that solution with previous cost function.

5.3.5 History of secondary system motion with new primary system motion

Since primary system solution shows better result with follow mocap cost function, it is expected that the secondary system shows better result as well. The secondary system motion is plotted with three different time step: 0.1 sec, 0.01 and 0.0001sec .

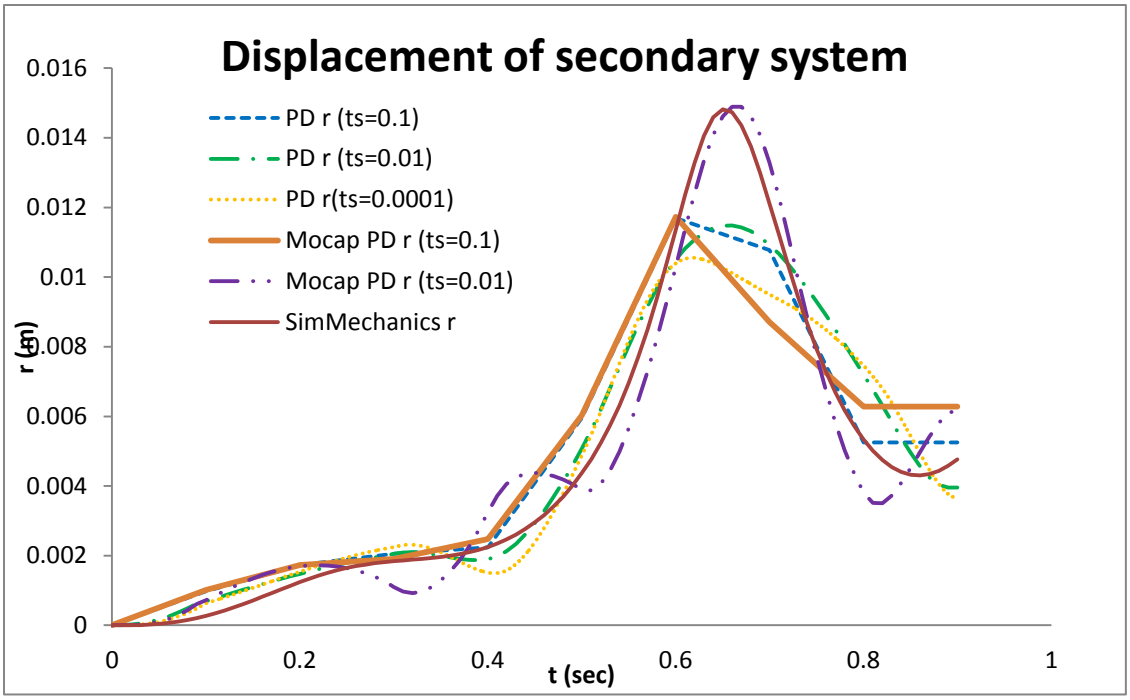

a) Comparison of displacement of secondary system

Figure 5-11 Comparison of calculated solution and benchmark solution with new primary system motion

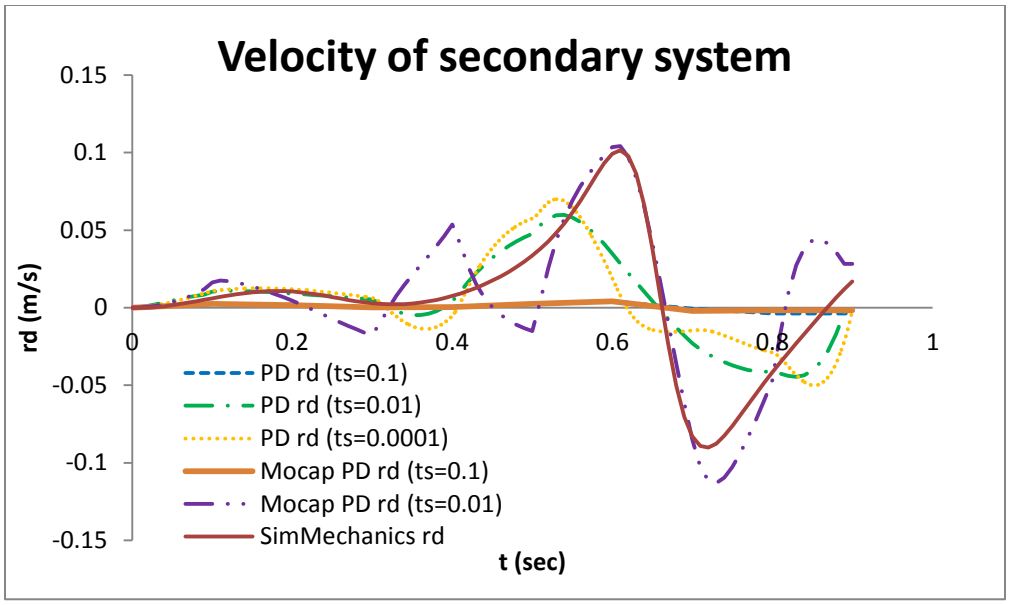

b) Comparison of velocity of secondary system

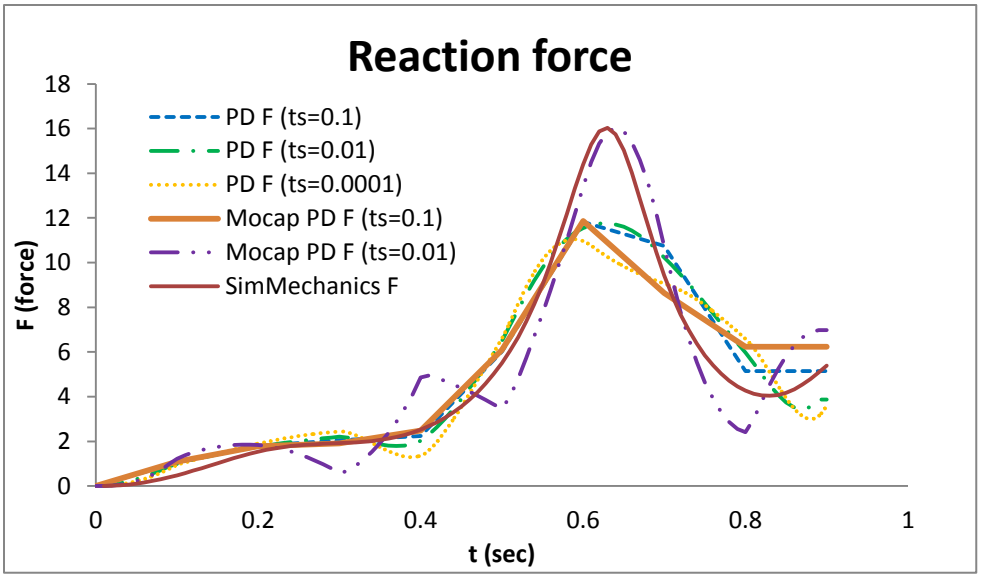

c) Comparison of reaction force on primary system due to the presence of secondary system

Figure 5-11 continued

When the primary system is solved with 0.1 and 0.01 time step, the plots are not smooth as much as the plots with 0.0001 time step. Again, the solution with new follow mocap cost function shows better result than the solution with old cost function. As a result, secondary system motion shows the best result by using new follow mocap function and 0.0001 sec for time step.

CHAPTER 6

CONCLUSIONS AND FUTURE WORK

In this dissertation, a method to simulate the human motion and the motion of external equipment while accounting for the cause and effect of the motion of equipment on the human was developed and presented. Since human body is composed of lot of links and degree of freedoms, the derivation and subsequent solution of equation of motion is a complicated task. Once the results are validated for simulation of human, whenever an equipment gets added, removed or moved, the equations of motion need to be re-derived. The re-derivation may also need re-validation once the model is implemented. Consequently, the equation of motion needs to be derived and solved only for specific attachment point on the body. This may not be a feasible option, especially if adding or removing or modifying location of the equipment is done frequently and by the end user. Moreover the approach being used for solving the human system is predictive dynamics, the procedure has to work with the predictive dynamics approach.

6.1 Conclusions

The proposed approach is to solve primary system and secondary system separately and observe interaction between two systems. To test and validate the developed approach, the upper and lower arms are simplified as two-link pendulum and external equipment is modeled as spring-mass-damper system. Since the kinematic information is obtained based on predictive dynamics module at each time, the equation of motion of secondary system is solved for the known input motion of the reference point (attachment point). After solving the secondary system, the reaction forces and moment are calculated at the attachment point. Based on the understanding of interaction forces from the equations of motion of coupled and independent systems, the reaction force is equivalent to sum of spring force and damper force because the secondary system

is one dof system. A global force corresponding to the reaction force is calculated and applied to the primary system as an external load in the predictive dynamics approach.

As a result, the interaction of the two systems including motion, reaction forces, and moment between the human body and the equipment are calculated and the effect of external forces on human motion is predicted. Since we use kinematic information at the attachment point of the primary system to analyze the secondary system, there is no need to derive equations of motion of primary system again although the attachment point is changed. Moreover, multiple equipment can be attached with relatively less computation and at any location on the human body.

The results of the reaction force and motion of the secondary system are compared with the benchmark solution from MATLAB/SimMechanics and the calculated results show good trend with proposed modeling approach.

6.2 Discussion and Future work

While a novel method of simulating the motion of the human and equipment mounted on human forces has been presented in this work, it opens up many interesting avenues of research that can be pursued in the future. For instance, Chapter 5 reports the comparison of the reaction force and secondary system motions. The calculated result shows error because it is assumed that $\theta_i, \dot{\theta}_i$ and $\ddot{\theta}_i$ are constant for given time instant, equation of motion is solved as nonhomogeneous ODE problem. It depends on time step to solve predictive dynamics module. Therefore, the error could be reduced by using other solution technique such as numerical integration.

Moreover, currently the secondary system has only one translational degree of freedom. To develop more accurate and natural motion, the secondary system should have rotational degree of freedom as well. Furthermore, the developed method is applied to only 2D problems in this dissertation; it should be applied and extended to the model including 3D motion of external equipment with rotation.

In addition, the presented method should be applied to a large dof digital human model. With human modeling simulation, the secondary system can be attached to different point on the human body with different orientations of multiple secondary systems. Hence the approach should be rigorously tested and then applied to a full digital human model with multiple equipment.

REFERENCES

Abdel-Malek, K., Arora, J., Frey Law, L., Swan, C., Beck, S., Xia, T., Bhatt, R., Kim, J., Xiang, Y., Rasmussen, M., K., Murphy, C., Laake, A., Mathai, A., Marler, T., Yang, J., and Obusek, J. (2008, June). *Santos: A digital human in the making*. presented at the IASTED International Conference on Applied Simulation and Modeling, Corfu, Greece.

Fisette, P., Pé terkenne, J.M.,1998. "Contribution to parallel and vector computation on multibody dynnamics". *Parallel Computing*, 24,pp.717-728, Elsevier

Gruber, K.,Ruder, H., Denoth, J.,Schneider, K.,1998. "A comparative study of impact dynamics: wobbling mass model versus rigid body models". *Journal of Biomechanics*, 31,pp.439-444, Elsevier

Lankarani, H.M., and Pereira, M.S., "Treatment of Impact with Friction in Open- and Closed-Loop Planar Multibody Systems" *International Journal of Multibody System Dynamics*, Vol. 6, pp. 203-227, 2001.

Renouf M, Acary V, Dumont G. 3D Frictional contact and impact multibody dynamics: A comparison of algorithms suitable for real-time applications. In: Goicolea JM, Cuadrado J, Garcia Orden JC, editors. Multibody dynamics 2005, ECCOMAS thematic conference. 2005.

Schiehlen, W., 1997. "Multibody system dynamics: Roots and perspectives". *Multibody System Dynamics*, 1, pp. 149-188, Kluwer Academic publishers

Verros, G., Natsiavas, S., 1999. "Forcing induced asymmetry on dynamical systems with cubic non-linearities". *Journal of Sound and Vibration*, Volume 221, Issue 5, Pages 823-848, Elsevier

Xiang, Y., Arora, J.S., Abdel-Malek K., 2009. "Optimization-based motion prediction of mechanical systems: sensitivity analysis". *Structural and Multidisciplinary Optimization*, Volume 37, Pages 595-608, Springer-Verlag

Xiang, Y., Chung, H., Kim, J.H., Bhatt, R., Rahmatalla, S.,Yang J., Marler, T. Arora, J.S.,Abdel-Malek K., 2010. "Predictive dynamics: an optimization-based novel approach for human motion simulation", *Structural and Multidisciplinary Optimization*, Volume 41, Pages 465-479, Springer-Verlag